GEOCHEMICAL STUDY OF LAVA FLOWS, EJECTA AND PYROCLASTIC FLOW FROM THE KRAKATAU GROUP, INDONESIA

Rep. Fac. Sci., Kagoshima Univ. (Earth Sci., Biol.),
No. 15, p. 41–76, 1982.

GEOCHEMICAL STUDY OF LAVA FLOWS, EJECTA AND PYROCLASTIC FLOW FROM THE KRAKATAU GROUP, INDONESIA

By

Noboru ŌBA*, Katsutoshi TOMITA*, Masahiko YAMAMOTO*, Mohamad ISTIDJAB**, M. BADRUDDIN**, M. PARLIN**, SADJIMAN**, Arief DJUWANDI**, Adjat SUDRADJAT*** and Totong SUHANDA***

(Received July 1, 1982)

Abstract

Geochemical and lithological studies of volcanic rocks, ejecta and pyroclastic flow, those of which were collected from the Krakatau Group, Anak Krakatau, Small Rakata, Rakata and Sertung, locating in the Sunda Strait waters between Sumatra and Jawa, were carried out. Phenocrystic minerals from the volcanic rocks were also investigated by the electron-probe microanalyzer. Thermally altered products and related minerals, and pyroclastic flow and ejecta were examined by the X-ray powder diffraction method and the scanning electron microscope.

Rocks and ejecta of Anak Krakatau apparently represent almost the same characteristic features not only lithologically but also geochemically, common to basaltic andesites of typical volcanoes of island arcs. Phenocrystic olivines, clinopyroxenes and orthopyroxenes are similar in chemical composition to those of volcanic rocks of island arcs and oceanic islands. It is noted that a new volcanic ash has some conspicuous difference; the ash is more basic in chemical composition than the volcanic rocks.

Volcanic rocks from Rakata can lithologically be distinguished into three rock types; augite-hypersthene andesite with the hyalopilitic texture of lava flow, augite andesite with the intergranular texture of lava flow, and olivine basalt with the intersertal texture of dike. It became clear that in mineral composition the rock having been called tridymite andesite which looks rhyolite at a glance is augite-hypersthene andesite with cavities filled with tridymite, which was identified by X-ray powder diffraction analysis.

Pyroclastic flow, which is believed to have been formed in the 1883 Krakatau eruption, is characterized by a large amount of volcanic glass being in a vesiculating state that gases were expanding and escaping, and by the high-contents of SiO_2, Na_2O and K_2O, while by the low-contents of MgO, FeO and CaO; it is lithologically andesitic and geochemically dacitic.

Granitic xenoliths of quartz monzonite in mineral composition were found from the pyroclastic flow of Sertung. From several evidences, it should be considered that the granitic xenoliths came from the underlying complex at depths, where the xenoliths were captured as foreign materials by the magma, from which the pyroclastic flow would have been produced. Meanwhile, the pyroclastic flow signifi-

* Institute of Earth Sciences, Faculty of Science, Kagoshima University, Kagoshima, Japan.
** Geochemical Laboratory, V.S.I., Yogyakarta, Indonesia.
*** Volcanological Survey of Indonesia, Bandung, Indonesia.

cantly differs in both mineral and chemical compositions against all volcanic rocks of the Krakatau Group. Thus, it may possibly be considered that the pyroclastic flow might have been related with the underlying granitic complex with respect to the generation of its source magma.

Introduction

The famous Krakatau eruption took place in 1883. A great huge amount of the materials was ejected out. It is well known that the ejecta travelled repeatedly around the globe. Due to the great eruption, the Sumatra and Jawa sea-coasts were completely destroyed and approximately 36,000 people were killed by th tsunami reaching a height of 30 m (SUDRADJAT, 1981).

Some of calderas of Japan, such as Aira and Ata, Kagoshima, South Kyushu, are believed to have had such a great eruption called "Krakatau-type". Therefore, geochemical study of the Krakatau Volcano and its related caldera will be worthful to make comparison with these calderas and related volcanoes, and to obtain the informations concerning the mechanisms of eruption and magma generation.

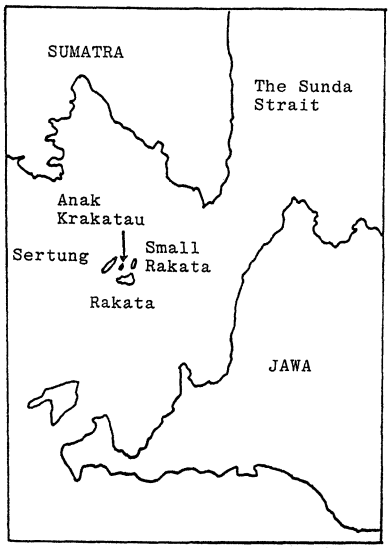

Fig. 1. Location of islands of the Krakatau Group.

Geological survey and collection of samples were made in 1981 at islands of Anak Krakatau, Small Rakata, Rakata and Sertung, those of which are located in Sunda Strait between Sumatra and Jawa (Fig. 1). These four islands have as a whole been called Krakatau volcano complex, Krakatau island complex or Krakatau volcano island complex (SUDRADJAT, 1981), and the Krakatau group (DE NÉVE, 1981b). In convenience, simple the Krakatau Group will be used in this paper for the whole islands.

Courses where geological surveys were taken and localities where samples were collected at the Krakatau Group are shown in Figs. 3 and 5. Following to the field work, analyses of mineral and chemical compositions, and X-ray studies, differential thermal analysis, scanning electron microscopy and infrared absorption spectra have been carried out for rocks of lava flows, ejecta, pyroclastic flow, thermally altered products and related minerals and others. Major attention will be given in this paper to the geochemical and lithological natures of these volcanic products.

Development history of the Krakatau Group

Development history of the Krakatau Group has recently been reported by DE NÉVE (1981a, b) and SUDRADJAT (1981) from its morphological aspects. According to

SUDRADJAT (1981), it will briefly be summarized as follows. Schematic models looking southeast-wards of the Krakatau Group showing its development history of the pre- and post–1883 eruption are presented in Fig. 2.

It was assumed that in the very early stage a gigantic stratovolcano, called "Ancient Krakatau Volcano" (ESCHER, 1919, cited from SUDRADJAT, 1981) (Fig. 2, A), of approximately 10~12 km in diameter and 2,000 m high rose in the Sunda Strait waters.

A plinian type-eruption took place and destroyed the volcano itself leaving the ruin of three islands; Rakata, Sertung and Panjang (Fig. 2, B) several centuries before. An ancient caldera with 7 km in diameter was formed at the third century AD (DE NÉVE, oral communication, 1981, cited from SUDRADJAT, 1981).

Volcanic activities presumably of vulcanian type continued and built up a stratovolcano, called Rakata Volcano of the pre-1883 eruption, with approximately 5 km in diameter and 800 m in height (Fig. 2, C). The volcanic activities at the Rakata Volcano shifted northwest-wards to the center of the ancient caldera and produced two volcanoes, Danan and Perbuatan, around 15 centuries. An island combined with three

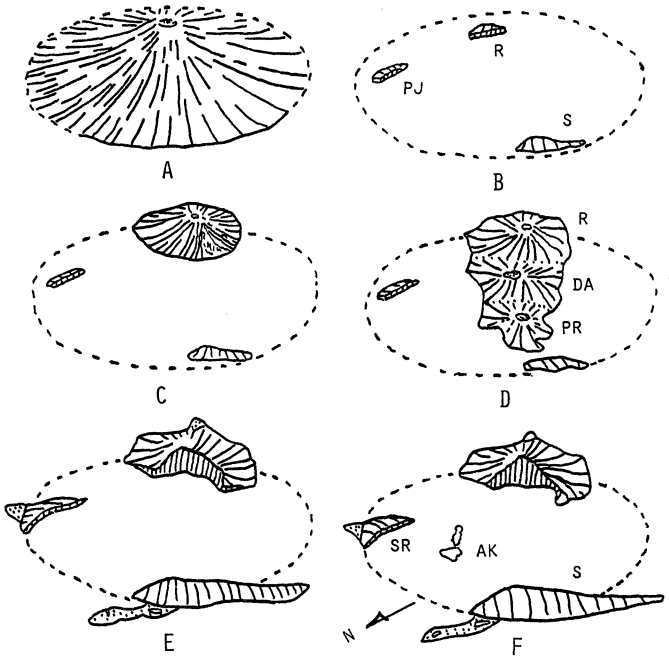

Fig. 2. Schematic models looking SE-wards of the Krakatau Group showing its development history of the pre- and post–1883 Krakatau eruption. A. Ancient Krakatau Volcano. B. The plinian type erutpion took place and destroyed the volcano leaving the ruin of three islands, Rakata (R), Sertung (S) and Panjang (PJ). An ancient Krakatau caldera was formed. C. Volcanic activity continued at Rakata. D. Glowing up of Rakata (R) before the 1883 Krakatau explosion. Volcanic activities shifted NW-wards the center of the ancient Krakatau caldera and produced two volcanoes, Danan (DA) and Perbuatan (PR). An island combined with three volcanic bodies was referred to as "Krakatau" of the pre–1883 eruption. E. Two volcanoes of Danan and Perbuatan and a portion of Rakata burst out and a new caldera occurred NW of Rakata in the 1883 explosion. F. Birth and growth of Anak Krakatau (AK). SR: Small Rakata. Figures after SUDRADJAT (1981).

volcanic bodies was sometimes referred to as "Kratkatau" of the pre–1883 eruption (Fig. 2, D).

At the 1883 eruption, two volcanoes of Danan and Prbuatan and a portion of Rakata Volcano were burst out (Fig. 2, E). A caldera with a depth of more than 250 m occurred northwest of Rakata Island. The submarine crater formed after the 1883 eruption was measured approximately 9~10 km in length and about 2 km in width at the depth of 100 m below sea-level.

During the period from 1883 to 1919, no significant change occurred at the sumbarine bottom of the caldera crater. After 1919, the northeastern upper inner slope of the submarine crater was being filled by the volcanic deposits produced by the newly born submarine Anak Krakatau Volcano.

Steaming of several ten meters high was first noticed in 1927 and a new volcano island with 8~10 m in diameter and 8.93 in height, like a sand-dune, Anak Krakatau, i.e., Child of Krakatau, was born and its growing up continued by 1930 (Fig. 2, F).

The volcano had the stages of the development and destruction during the period from 1930 to 1950. A new volcanic cone was born in 1950 as an inner cone, i.e., a parasit cone, within the outer ring of the volcano. The new inner cone has been characterized by the lava-outpuring since the 1960–1963 period. At the present time, the summit of the inner cone achieves 199.29 m in height and that of the outer cone 151.66 m in height above sea-level.

As seen from the above-mentioned, a steeply inclined wall forming the northern seacoast of Rakata Island (Fig. 15, C), which is the remnant of the past "Krakatau", shows a portion of the caldera wll formed at the 1883 eruption, and it seems that the submarine calderas or craters duplicated by the ancient caldera and the 1883 caldera may exist within the submarine bottom surrounded by the present three islands.

Geology

1. Anak Krakatau

Anak Krakatau Volcano Island, for which simple Anak Krakatau will be used here, is composed of two main parts; an outer cone and an inner cone, a parasit cone (Fig. 13, B and C), which was born within the outer ring. That is, the volcano is a double cone. The activity of Anak Krakatau is characterized by the lava-outpouring in 1960~1963, 1972~1973, 1975 and 1979 (SUDRADJAT, 1981). At present, the frequent summit eruption of volcanic ejecta with gases at the crater of the inner cone is continuing (Fig. 13, A).

Geologic map of Anak Krakatau was tentatively compiled from a map showing the distribution of lava flows, received in 1981 from Volcanological Survey of Indoensia, and a geologic map made by this work. A map showing the distribution of 1972~1973 lava flow and 1975 lava flow, reported by R.D. HADISANTONO and L. PARDYANTO (Volcanol. Soc. Japan and IAVCEI, 1980), and a sketch of 1979 lava flow by D. SUMPENA (Volcanol. Soc. Japan and IAVCEI, 1981) were also referred. The compiled

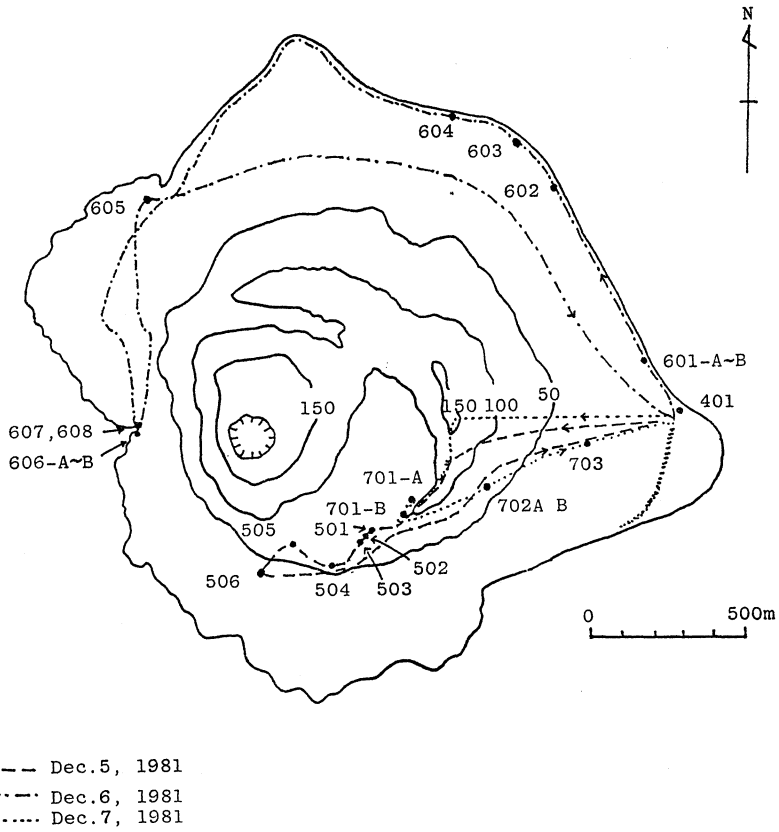

Fig. 3. Courses where geological surveys were made at Anak Krakatau. Solid circles and numbers represent localities where samples were collected.

distribution map of 1963, 1972–1973, 1975 and 1979 lava flows is shown in Fig. 4. The 1972 lava flow and the 1973 lava flow are drown as the 1972–1973 lava flow on the map, because the boundary between them could not be settled in 1981. The mode of occurrence of the 1972–1973 lava flow is shown in Fig. 14, C.

(1) Outer cone

On the steep crater wall in the western inside of the outer ring, one yellow-colored and layered deposit, which looks like a lava flow, was observed (Fig. 14, A). As a result of a field observation, this was not a lava flow, but a stratified deposit of thrown-out debris, i.e., a pyroclastic deposit, which strikes N 40°E and dips 20°E and is 7 m in thickness, composed mainly of scoria (Fig. 14, B). This is called, in convenience, the yellow-colored and stratified pyroclastics in this paper. Most of scoria are 1~5 cm in diameter, and the maximum in size 30 cm.

It is not certain whether the whole body of the outer cone above sea-level is interculated with a lava flow. There is a report that a newly born Anak Krakatau has had a sand dune-like shape (SUDRADJAT, 1981). Judging from the fact that the whole of the steep crater wall in the western inside of the outer ring is made up of the stratified pyroclastics and no lava flow is observable, the outer cone may possibly be a pryoclastic cone.

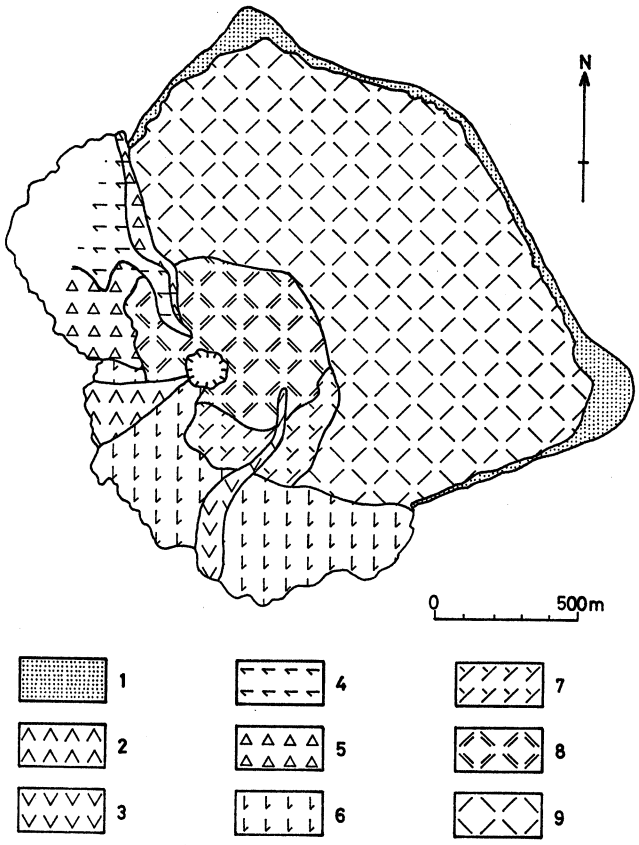

Fig. 4. Geologic map of Anak Krakatau, compiled from the published geologic maps and this work. Stratigraphic sequence: 1, Alluvial deposits; 2. 1979 lava flow; 3, Lava flow of unknown age; 4, 1975 lava flow; 5, 1975 (?) lava flow; 6, 1972–1973 lava flow; 7, 1963 lava flow; 8, Scoria and lithic block of the inner cone; 9, Scoria and lithic block of the outer cone.

A large number of thread bomb, bread-crust bomb and lithic bomb are observed on the eastern slope of the outer cone. An ellipsoidal bread-crust bomb, one of them, as shown in Fig. 14, D, reaches nearly 2 m in an elongated diameter. This bomb is thought to be one itself which was reported from the Scientific Event Alert Network, NHB9, Smithonian Institution, Washington, D. C., U.S.A. (GEOTIMES, 1979), that is, the bomb which fell as far away as 400 m from the crater at the end of September, 1979.

On the eastern foot and along the southeast-seacoast of the outer cone, fall deposits composed mainly of scoria and volcanic sand are developed (Fig. 14, E).

(2) Inner cone

Volcanic activity of bulcanian type, represented by both the summit frequent eruption of volcanic ejecta with gases and lava-outpouring, at the inner cone is similar to that of Sakurajima Volcano, locating on the rim as a central cone within the Aira caldera, Japan. The volcanic activity of Sakurajima Volcano has containued for 26 years since 1955. Lava flows of Anak Krakatau are blocky and sometimes very porous, then some are aa-type.

2. Samall Rakata, Rakata and Sertung

Three islands of Small Rakata, Rakata and Sertung facing towards Anak Krakatau, roughly speaking, correspond to the caldera wall of the ancient Krakatau Volcano or the 1883 Krakatau Volcano (Fig. 2). A steeply inclined wall seen at the northern seacoast

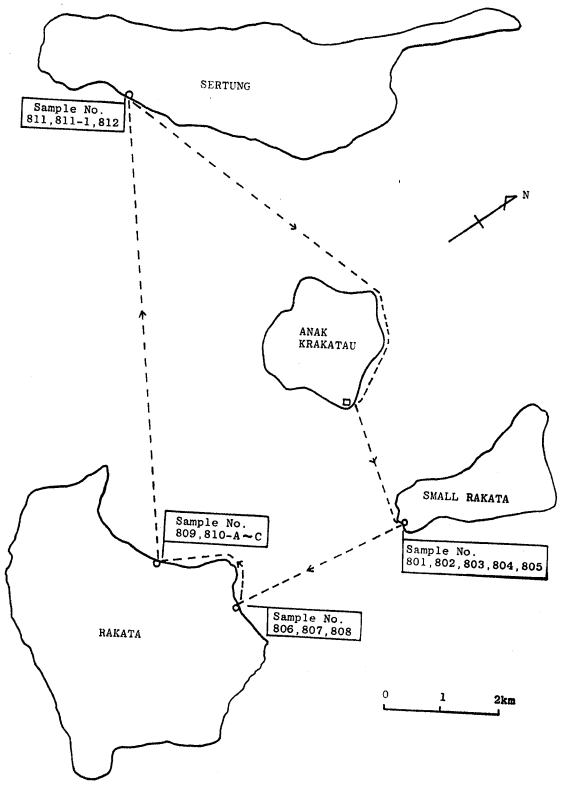

Fig. 5. Courses where geologic inspections were taken and localities where samples were collected at each islands, Small Rakata, Rakata and Sertung, of the Krakatau Group.
Numbers are collected sample no.

of Rakata typically represents the remnant of the 1883 Krakatau explosion caldera.

Such a relation is, as a whole, quite similar to a relation between Sakruajima active volcano and its surrounding caldera wall of the Aira caldera which is believed to have had the so-called "Kratakatau-type eruption". Submarine volcanoes with craters are present within the Aira caldera which is filled by sea-wster. One of them is still active and has fumaroles emanating volcanic gases of high temperature.

Therefore, the geochemical comparison between both the Krakatau caldera and its related Anak Karakatau active volcano and both the Aira caldera and its related Sakurajima active volcano will be worthful to obtain the informations concerning the mechanism of eruption and magma generation.

Pyroclastic flow ejected out in the 1883 Krakatau explosion occurs at Small Rakata, Rakata and Sertung, and overlays the basement complex composed mainly of volcanic rocks, most of which are lava flows of basaltic andesite, of these islands. It is very similar to the so-called "Shirasu" pyroclastic flow prevailing over South Kyushu, Japan, in many respects such as petrographic appearance and constituent materials.

(1) Small Rakata

According to the geologic map, received in 1981 from Volcanological Survey of Indonesia, Small Rakata Island (Fig. 14, F) consists of tridymite andesite, which makes the basement of the island, and the products of the 1883 Krakatau eruption.

At the point where samples of nos. 801–805 were collected at the seacoast in the

southern most of the island (see Fig. 5), agglutinate lava flow (Fig. 15, A), which strikes N 50°W and dips 30°S, of olvine-bearing hypersthene-augite andesite occurs and is overlaid by pumice fall of 10 m in thickness. The pumice fall is overlaid by pyroclastic deposit of 2 m in thickness, which lies under pyroclastic flow (Fig. 15, B) of about 20 m in thickness. The pyroclastic flow is the product of the 1883 Krakatau eruption. Both the pyroclastic deposit and the underlying pumice fall are unknown at present in their relationship.

(2) Rakata

According to the geologic map from Volcanological Survey of Indoenisa, Rakata Island (Fig. 15, C) geologically consists of the basement complex, comprising basalt, tridymite andesite and hypersthene andesite, and of the products of the 1883 Krakatau eruption.

At the point where samples of nos. 806~808 were collected at the seacoast facing north of the NNE-side of Rakata (see Fig. 5), dark grey-colored augite-hypersthene andesite with cavities filled by tridymite crystal (sample no. 806) of lava flow which looks like rhyolite at a glance is exposed. Some blocks of black-colored olivine basalt (sample no. 807) are observed.

Meanwhile, at the point where samples of nos. 809 and 810–A~C were collected at the seacoast facing northwest of the northwestern side of the island (see Fig. 5), many dikes of olivine basalt (sample no. 810–A~C) which cut lava flow of augite andesite (sample no. 809) can be observed (Fig. 15, D and E).

(3) Sertung

According to the geologic map from Volcanological Survey of Indoensia, Sertung Island (Fig. 15, F) is geologically composed of the basement complex, which comprises tridymite andesite and hypersthene andesite, and of the products of the 1883 Krakatau eruption which overlays the basement complex.

At the point where samples nos. 811~812 were collected at the southeastern seacoast of the island (see Fig. 5), agglutinate lava flow of olivine-hypersthene-augite andesite (sample no. 812) and pyroclastic flow (Fig. 15, G) (smaple no. 811) with a bed of pumice fall are observed. A schematic model showing a geologic relation among them is given in Fig. 6.

The agglutinate lava flow is 30 m in thickness on appearance at the exposure and occupies a main portion of the basement of the island. The pumice fall, stratified air fall deposit, of 2 m in thickness overlays the basement lava flow and lies under the pyroclastic flow. Pumice is 10~20 cm in diameter at the lower part and 1~5 cm in

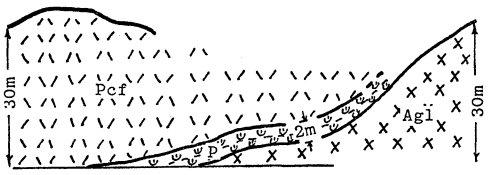

Fig. 6. Schematic model showing a geologic relation between agglutinate lava flow (Agl), pumice fall (P) and pyroclastic flow (Pcf) at the SE-seacoast of Sertung.

diameter at the upper part of the bed. The pyroclastic flow is non-stratified massive here and about 30 m in thickness. The pumice fall is the preceeding product prior to the successive great eruption accompanied by a huge amount of the pyroclastic flow in 1883. As will be discussed later, granitic xenoliths were found from the pyroclastic flow.

Petrography

Thirty eight samples, in which twenty three from Anak Krakatau, five from Small Rakata, seven from Rakata and three from Sertung, of rocks of lava flows, ejecta, pyroclastic flows, thermally altered products and others were collected at the Krakatau Group for geochemical investigations. Sample no., localities and rock types of collected samples are listed in Table 1.

Thin sections were made of fifteen samples of rocks, pyroclastic flow, volcanic ash and others in question for microscopic examination. Another thin sections more than five were prepared for chemical analysis of phenocrystic minerals by means of the electron-probe microanalyzer (EPMA).

Table 1. Rock types and localities of samples collected from the Krakatau Group

SAMPLE NO.	LOCALITIES	ROCK TYPES	NOTE
401 (c)	Anak Krakatau	Volcanic ash and scoria	
501 (*,c)	Anak Krakatau	Olivine-bearing hypersthene-augite andesite	1963 lava
502	Anak Krakatau	Altered basaltic andesite	White-colored hydrothermally altered 1963 lava
503	Anak Krakatau	Altered basaltic andesite	Yellow-colored hydrothermally altered 1963 lava
504 (*,c)	Anak Krakatau	Olivine-bearing hypersthene-augite andesite	1972 or 1973 lava
505	Anak Krakatau	Altered basaltic andesite	Hydrothermally altered 1963 lava
506	Anak Krakatau	Basaltic andesite	Lava of unknown age
507	Anak Krakatau	Basaltic andesite	1972 or 1973 lava
601-A	Anak Krakatau	Lapilli and block	Stratified pyroclastics; coarse grain in size
601-B	Anak Krakatau	Scoria	Stratified pyroclastics; fine grain in size
602	Anak Krakatau	Metamorphosed tuff (?)	Block at beach
603	Anak Krakatau	Tuffaceous sandstone	Block at beach
604	Anak Krakatau	Tuffaceous sandstone	Xenolith within andesite; block at beach
605 (*,c)	Anak Krakatau	Olivine-hypersthene-augite andesite	1975 lava
606-A	Anak Krakatau	Basaltic andesite	1972 or 1973 agglutinate lava (?)
606-B	Anak Krakatau	Basaltic andesite	1972 or 1973 agglutinate lava (?); red-colored
607	Anak Krakatau	Basalt	Bread-crust bomb
608	Anak Krakatau	Tuffaceous sandstone	Block at beach
701-A	Anak Krakatau	Scoria	Yellow-colored stratified pyroclastics

Table 1. (Continued)

SAMPLE NO.	LOCALITIES	ROCK TYPES	NOTE
701-B	Anak Krakatau	Scoria	Yellow-colored stratified pyroclastics
702-A (*,c)	Anak Krakatau	Olivine-bearing hypersthene-augite andesite	Bread-crust bomb
702-B (*,c)	Anak Krakatau	Olivine-hypersthene-augite andesite	Xenolith within bread-crust bomb No. 702-A
703	Anak Krakatau	Basaltic andesite	Bomb
801	Small Rakata	Pyroclastic flow	Due to 1883 eruption
802	Small Rakata	Altèred andesite	Debris from pyroclastic rock
803	Small Rakata	Pyroclastic rock	Coarse grain in size; cross-laminated
804	Small Rakata	Pyroclastic rock	Fine grain in size; cross-laminated
805 (*)	Small Rakata	Olivine-bearing hypersthene-augite andesite	Agglutinate lava
806 (*)	Rakata	Augite-hypersthene andesite	With tridymite crystals
807 (*)	Rakata	Olivine basalt	Block
808	Rakata	Pumice	As a block
809 (*)	Rakata	Augite andesite	Intruded by dike No. 810-A~C
810-A	Rakata	Olivine basalt	Dike: east side-margin of dike No. 810-A~C
810-B (*)	Rakata	Olivine basalt	Dike: core of dike No. 810-A~C
810-C (*)	Rakata	Olivine basalt	Dike: west side-margin of dike No. 810-A~C
811 (*,c)	Sertung	Pyroclastic flow	Weakly welded; due to 1883 eruption
811-1 (*)	Sertung	Biotite granodiorite	From the 1883 pyroclastic flow
812 (*)	Sertung	Olivine-hypersthene-augite andesite	Unknown age
	Total 38 samples		

* represent those which thin-section was made for microscopic observation.
c represent those which chemical analysis was made.

Modal analyses of volcanic rocks of lava flows and dike from the Krakatau Group, and granitic xenolith from Sertung are tabulated in Tables 2 and 5. Mineral compositions, expressed by the relative abundance of minerals on appaearance, of volcanic ash from Anak Krakatau and pyroclastic flow from Sertung are given in Tables 3 and 4.

1. Anak Krakatau

A geologic map, compiled from the published geologic maps and this work, is shown in Fig. 4. Volcanic rocks are, as Table 2 shows, apparently basaltic andesites, represented by olivine-hypersthene-augite andesite of the 1975 lava flow (sample no. 605) and olivine-bearing hypersthene-augite andesites of the 1963 lava flow (sample no. 501) and the 1972–1973 lava flow (sample no. 504). Microphotograph of the rock of the 1963 lava flow, one of typical rocks, is shown in Fig. 16, A.

Phenocrystic minerals are plagioclase, augite, hypersthtne, olivine and titanom-

Table 2. Modal compositions (%) of volcanic rocks from the Krakatau Group

Island	AK	AK	AK	AK	AK	SR	R	R	R	R	S
Sample no.	501	504	605	702-A	702-B	805	806	807	809	810-B	812
Analyst	TI	TI	TI	TI	TI	TI	SK	SK	SK	SK	SK
Phenocryst											
Ol	1.5	1.0	1.3	0.4	1.2	0.1	n	6.0	n	3.7	1.7
Cpx	3.2	5.6	3.1	4.8	3.3	0.8	0.2	n	14.6	n	4.2
Opx	1.7	2.5	1.2	2.5	1.3	0.4	0.4	n	n	n	2.5
Ore	1.2	0.3	0.6	1.5	0.7	0.3	0.6	0.6	4.5	2.4	0.3
Pl	26.4	24.3	23.7	23.4	22.7	4.9	8.6	43.0	49.1	18.9	21.7
Others	0.5	0.8	0.3	0.5	0.4	n	0.2	n	0.2	n	n
Groundmass	65.5	65.4	69.8	66.9	70.5	93.6	90.0	50.4	31.6	75.1	69.5
Ol	n	n	n	n	n	n	n	+	n	n	n
Cpx	+	+	+	+	+	+	+?	++	+++	++	+
Opx	+	+	+?	+	+?	+?	+	?	n	+	+
Ore	+	+	+	+	+	+	+	+	+	+	+
Plm	++++	+++	+++	+++	+++	+++	+++	+++	+++	+++	++++
V	++++	++++	++++	++++	++++	++++	++++	+++	+	++	++++
Texture	hyal	hyal	hyal	hyal	hyal	pilo	hyal	inters	interg	inters	hyal

Abbreviations: AK, Anak Krakatau; SR, Small Rakata; R, Rakata; S, Sertung; TI, T. Ishii; SK, S. Kiyosaki; Ol, Olivine; Cpx, Clinopyroxene; Opx, Orthopyroxene; Ore, Opaque mineral; Pl, Plaigoclase; Plm, Plaigoclase microlite; V, Volcanic glass; hyal, hyalopolitic; pilo, pilotaxitic; inters, intersertal; interg, intergranular. Symbols representing the relative abundance of constitutent minerals of the groundmass: ++++>+++>++>+. n: Not observable.

agnetite. Ilmenite occurs only in the rock of the 1972–1973 lava flow. The groundmass is assembled by plagioclase microlite, augite, hypersthene, titanomagnetite, and brown volcanic glass, and has the hyalopilitic texture. Apatite is accompanied as an inclusion. Most phenocrystic olivines show the corroded form with the reaction rim consisting of aggregates of pyroxene and opaque mineral.

A xenolith of olivine-hypersthtne-augite andesite (sample no. 702-B), found from a bread-crust bomb of olvine-bearing hypersthtne-augite andesite (sample no. 702–A) which is thought to be the bomb ejected in 1981, is quite different in its texture of the groundmass from both its host rock and other rocks of lava flows; the xenolith does not porous, but dense and much more glassy.

A new volcanic ash, collected on December 4, 1981, at the eastern seacoast of the outer cone, as Table 3 shows, is composed of plagioclase, hypersthene, augite, a small amount of olvine and ore mineral and a large amount of volcanic glass. That is, major mineral constituents of the volcanic ash are essentially the same as those of most volcanic rocks of Anak Krakatau. The followings are char-

Table 3. Mineral composition of volcanic ash from Anak Krakatau

Sample no.	401
Ol	+
Opx	++
Cpx	++
Ore	+
Pl	+++
V	++++

Abbreviations and symbols are the same as those in Table 2.

acteristic: the presence of plagioclases in which micrograins of brown-colored volcanic glass are arranged parallel to cleavage; and the presence of volcanic glasses containing small bubbles which show that gases were expanding.

2. Small Rakata

Rock of agglutinate lava flow (sample no. 805), which is thought to be one of the basement constituents of Small Rakata Island, is olivine-bearing hypersthene-augite andesite. Under the microscope, the rock is characterized by the distinctive structure looking an amygdaloidal pattern, while the groundmass of the rock has the pilotaxitic texture characterized by felted microlites in glassy matrix (Fig. 16, B).

In part of the groundmass, there are observed xenoliths showing an intergranular texture consisting of phenocrystic minerals and interstitial augite micrograins which fill lath-shaped plagioclase microlites (Fig. 16, C). The phenocrystic minerals and the groundmass texture of the xenoliths are quite the same as those of augite andesite, sample no. 809, from Rakata. This fact suggests that the xenoliths were captured from the underbeneath, where augite andesite may have been one of the constituents of the Krakatau Volcano before the present Rakata or the ancient Krakatau Volcano.

Pyroclastic flow which occurs at Small Rakata will be discussed later in connection with that of Sertung. X-ray data and observation by the scanning electron microscope of pumice fall, which is interculated between the agglutinate lava flow and the pyroclastic deposit under the pyroclastic flow, will also be given later.

3. Rakata

Augite-hypersthene andesite (sample no. 806)

Rock collected at the north-seacoast of Rakata has been called tridymite andesite and looks rhyolite at a glance at the exposure. Phenocrystic minerals are, however, plagioclase, hypersthene, augite and opaque mineral, and the groundmass has the hyaloplitic texture (Fig. 16, D). Accordingly, the rock is, in mineral composition, augite-hypersthene andesite with cavities filled with tridymite crystal, but not rhyolite. Crystals filling cavities, like druths, developed in the rock were determined by the X-ray powder diffraction analysis to be tridymite.

Augite andesite (sample no. 809)

Rock of lava flow, which occurs at the northwest-seacoast of Rakata is characterized by phenocrystic plagioclase and augite, and the groundmass showing an intergranular texture (Fig. 16, E) composed of lath-shaped plagioclase microlite and interstitial augite micrograin; that is, the rock is augite andesite. The lava flow of this rock is intruded by many dikes (Fig. 15, D), one of which is olivine basalt (Fig. 15, E).

Olivine basalt (sample nos. 810-B and 807)

Rock sample, no. 810–B, collected from the core part of a dike (Fig. 15, E), which cuts augite andesite lava flow at the northwest-seacoast of Rakata, was examined under the microscope. The rock is olivine basalt characterized by abundant phenocrystic olivine and the groundmass giving the intersertal texture that lath-shaped

plagioclase microlites are interstitially filled by micrograins of pyroxene and volcanic glass (Fig. 16, F).

Rock collected from a block at the north-seacoast of Rakata (sample no. 807) is lithologically quite the same as olivine basalt (sample no. 810–B) of the dike which occurs at the northwest-seacoast of the same island not only in mineral composition, but also in the texture of the groundmass. Thus, it is clear that the block came from either the extention of the same dike or one of dikes which have the same lithological feature.

4. Sertung

Pyroclastic flow (sample no. 811)

Light grey~white-colored pyroclastic flow was sampled at Sertung. Pumices of 2~3 cm in diameter are contained as the essential material in the pyroclastic flow, but not so abundant. The matrix of the pyroclastic flow is quite the same as pumice itself in mineral composition. Granitic xenoliths are contained, as will be mentioned later. In the pyroclastic flow at Small Rakata, altered andesitic xenoliths are also contained.

The pyroclastic flow is, as Table 4 shows, composed of plagioclase, hypersthene, augite, a large amount of volcanic glass with microlite, and a small amount of ore mineral. An accompanying apatite as an inclusion is present. That is, the pyroclastic flow is andesitic in mineral composition.

Table 4. Mineral composition of the 1883 pyroclastic flow of Sertung

Sample no.	811
Orthopyroxene	+
Clinopyroxene	+
Ore mineral	+
Plagioclase	+++
Volcanic glass	++++

Symolbs are the same as those in Table 2.

Most of volcanic glasses are colorless and transparent irregular shaped flakes and splits, and some are dusty and brown-colored volcanic glasses. As shown in the scanning electron microphotographs (Fig. 17, A~D) taken for fractions less than 2 μm in size, the volcanic glasses occur in such a form as acicular and fibrous glasses, and vesicle- and tube- or hole-bearing glasses. Many tubes or holes observed within the volcanic glasses show the fact that gases passed through.

Granitic xenoliths found from pyroclastic flow

One granitic xenolith (sample no. 811–1), holocrystalline in texture, of 5 cm in diameter was found from the pyroclastic flow at the southeast-seacoast of Sertung. Later, another one grain of 2 mm in size of granitic xenolith was found from the collected sample itself of the same pyroclastic flow at laboratory. This fact suggests that this kind of xenolith may be contained much more in the pyroclastic flow.

The granitic xenolith is composed of quartz, plagioclase, potash feldspar, biotite as chloritized pseudomorph, and opaque mineral. Apatite is accompanied as an inclusion. According to the classification and nomenclature of plutonic rocks by the

Table 5. Modal composition (%) of granitic xenolith found from the 1883 pyroclastic flow

Sample no.	811-1
Quartz	11.5
Plagioclase	54.0
Potash feldspar	24.9
Biotite, as chloritized pseudomorph	6.4
Ore mineral	3.1

Analyst: S. Kiyosaki.

IUGS Subcommission on the Systematics of Igneous Rocks (1973), as modal composition (Table 5) shows, the xenolith belongs to quartz monzonite.

The presence of many well-developed myrmekites, which appear typically in granodiorite, quartz monzonite and adamellite, is characteristic (Fig. 16, G). The myrmekite consists of intergrowth of quartz and plagioclase in the portion where plagioclase abuts on potash feldspar. Potash feldspars show dusty appearance in many cases. Quartz is not so abundant.

Mafic minerals are psuedomorphs after biotites, because most of mafic minerals show flakes elongated parallel to basal cleavage (Fig. 16, H). Primary biotites are converted into pale green chlorites with secondary magnetite-dust, and, sometimes, with zoisite micrograins also.

Olivine-hypersthene-augite andesite (sample no. 812)

Rock collected from lava flow which occurs at the southeast-seacoast of Sertung is olivine-hypersthene-augite andesite. Phenocrystic minerals are plagioclase, hypersthene, augite, and titanomagnetite as an opaque mineral. The groundmass has the hyalopilitic texture. The following features are characteristic: most phenocrystic plagioclases are saussuritized in their cores; some phenocrystic olivines are serpentinized in their borders, and very often along cleavages and cracks, and, sometimes, even in cores; and some phenocrystic pyroxenes are chloritized. These facts reveal that the rock was subjected to the weathering.

Geochemistry

1. Bulk Chemistry

Rocks of the 1963 lava flow (sample no. 501), the 1972–1973 lava flow (sample no. 504) and the 1975 lava flow (sample no. 605), one volcanic bomb (sample no. 702–A), one xenolith (sample no. 702–B) from the volcanic bomb (sample no. 702–A) and one volcanic ash (sample no. 401), those of which were collected at Anak Krakatau, and one pyroclastic flow (sample no. 811) collected at Sertung were chemically analyzed by a combination of the gravimetric method for SiO_2 and $H_2O\pm$, the colorimetric method for TiO_2 and P_2O_5, the atomic absorption method for Al_2O_3, total Fe, MnO, MgO, CaO, Na_2O and K_2O, and the volumetric method for FeO. The rocks and ejecta were pulverized by a vibrating mill and the pyroclastic flow was sieved under 32 mesh in particle and pulverized in advance for analysis.

Chemical analyses are given in Table 6, together with their CIPW normative

Table 6. Chemical analyses and CIPW norms of volcanic rocks from the Krakatau Group

Rock No.	501	504	605	702-A	702-B	401	811	*
SiO_2	53.74	54.74	53.76	54.38	53.72	52.60	65.22	53.41
TiO_2	1.04	0.99	0.83	1.10	1.05	1.01	0.71	0.79
Al_2O_3	17.95	17.56	18.15	17.88	18.01	17.81	14.18	17.75
Fe_2O_3	2.47	2.34	2.30	2.96	3.29	2.68	1.39	3.24
FeO	6.44	6.61	6.60	5.88	5.76	6.00	2.16	6.25
MnO	0.19	0.19	0.19	0.19	0.19	0.19	0.13	0.17
MgO	4.34	4.41	4.43	4.16	4.40	4.77	1.10	4.78
CaO	8.37	8.10	8.05	7.90	8.28	8.57	2.54	9.54
Na_2O	3.55	3.54	3.51	3.69	3.62	3.55	4.91	2.60
K_2O	0.84	0.85	0.88	0.93	0.81	0.76	2.15	0.68
H_2O+	0.58	0.36	0.77	0.49	0.48	1.41	4.76	0.48
H_2O-	0.02	tr.	tr.	0.04	tr.	0.12	0.58	0.23
P_2O_5	0.25	0.31	0.33	0.32	0.33	0.27	0.15	0.14
Total	99.78	100.00	99.80	99.92	99.94	99.74	99.98	100.06
Q	4.35	5.64	4.29	5.64	5.06	3.18	21.19	7.47
Or	4.96	5.02	5.20	5.50	4.79	4.49	12.71	4.02
Ab	30.04	29.96	29.70	31.23	30.63	30.04	41.55	22.00
An	30.56	29.52	31.17	29.48	30.50	30.42	10.30	34.76
Di Wo	3.89	3.61	2.78	3.18	3.52	4.32	0.55	4.87
Di En	2.11	1.93	1.46	1.83	2.10	2.52	0.31	2.81
Di Fs	1.65	1.57	1.22	1.21	1.24	1.59	0.22	1.84
Hy En	8.70	9.06	9.57	8.53	8.86	9.36	2.43	9.10
Hy Fs	6.78	7.36	7.99	5.67	5.24	5.90	1.67	5.97
Mt	3.58	3.39	3.33	4.29	4.77	3.89	2.02	4.70
Il	1.98	1.88	1.58	2.09	1.99	1.92	1.35	1.50
Ap	0.58	0.72	0.76	0.74	0.76	0.63	0.35	0.32

* Arithmetic mean of basaltic andesites of island arcs (EWART, 1976). Analyst: M. YAMAMOTO.

compositions. An arithmetic mean of basaltic andesites of island arcs by EWART (1976) is also given in the same table for comparison.

(1) Lava flows and ejecta of Anak Krakatau

As suggested from Table 6, apparently all rocks and ejecta from Anak Krakatau represent geochemically almost the same and simple characteristic feature, common to basaltic andesites of typical volcanoes of island arcs of western and northern Pacific and Caribbean regions (EWART, 1976).

The SiO_2-content of the analyzed rocks and ejecta ranges from 53 to 55 wt. %. According to the classification of volcanic rocks from active volcanic arcs and continental margins in the world (CARMICHAEL et al., 1974), the volcanic rocks and ejecta of Anak Krakatau are basaltic andesite in chemical composition. It is noted that the volcanic ash, which is believed to be a new ejecta at Anak Krakatau, has some conspicuous difference; the SiO_2-content and the value of normaltive quartz are lower as compared with those of lava flows and volcanic bomb.

Plotting of the analyzed volcanic rocks of Anak Krakatau on KUNO's (1966) SiO_2-(Na_2O+K_2O) diagram (Fig. 7) regarding the general boundaries between the tholeiite series, the high-alumina series and the alkali olivine-basalt series for the late Cenozoic

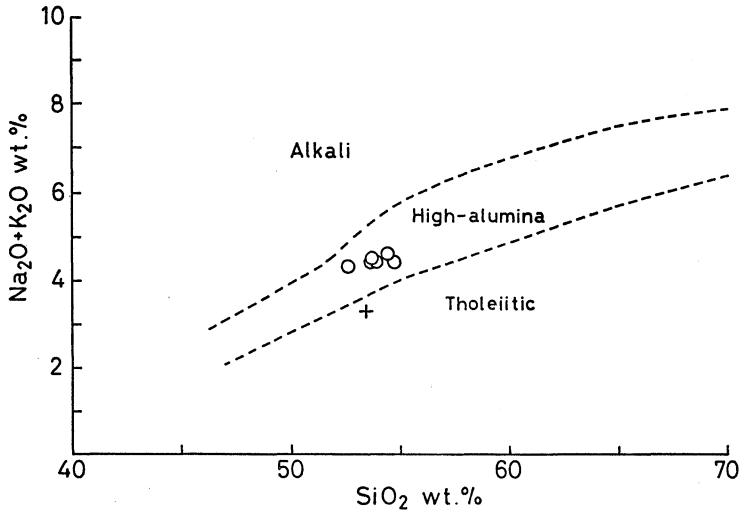

Fig. 7. Plots of the analyzed volcanic rocks of Anak Krakatau (open circles) on KUNO's (1966) SiO_2–(Na_2O+K_2O) diagram for the late Cenozoic volcanic rocks of the Japanese island arcs. Two dashed lins denote the general boundaries between the tholeiite series, the high-alumina series, and the alkali olivine-basalt series. Plus represents an average composition of basaltic andesites of typical volcanoes of island arcs of western and northefn Pacific and Carribean regions (data from EWART, 1976).

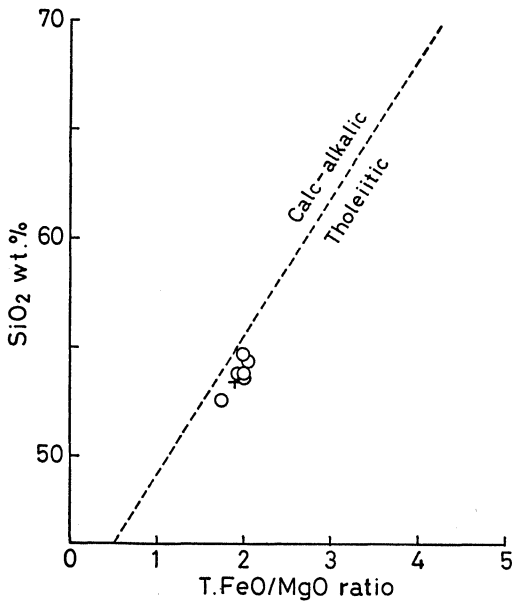

Fig. 8. Plots of the analzyed volcanic rocks of Anak Krakatau on MIYASHIRO's (1974) SiO_2-total FeO/MgO diagram. The dashed line represents the general boundary between the calc-alkalic rocks series and the tholeiitic series for non-alkalic volcanic rocks of western Pacific island arcs. Symbols are the same as those in Fig. 7.

volcanic rocks of the Japanese island arcs, the plots fall within a field of the high-alumina series. Taking account of the total FeO/MgO ratio against the SiO_2-content, the plots of the volcanic rocks of Anak Krakatau fall within a field of the tholeiitic series on MIYASHIRO's (1974) diagram (Fig. 8) regarding the general boundary between the calc-alkalic rock series and the tholeiitic series for western Pacific island arcs. In

CIPW normative composition, normative Q and Wo are calculated in all analyzed volcanic rocks of Anak Krakatau; the rocks are Q-normative and metaaluminous rocks. Besides, it is noted that the $Fe^{3+}/(Fe^{2+}+Fe^{3+})$ ratios of both the volcanic bomb and the xenolith from the same volcanic bomb are higher than those of the lava flows.

(2) Pyroclastic flow of Sertung

Pyroclastic flow collected at Sertung is significantly different in chemical composition from the volcanic rocks and ejecta of Anak Krakatau; characteristically the pyroclastic flow is rich in SiO_2 and alkalies, while, in contrast, poor in MgO, FeO and CaO. Naturally, a large amount of normative quartz and orthoclase are calculated. Thus, it can be said that in chemical composition the pyroclastic flow is dacitic.

2. Geochemistry of Phenocrystic Minerals

Phenocrystic olivines, clinopyroxenes, orthopyroxenes and plagioclases of volcanic rocks, sample nos. 501, 504, 605, 702-A and 702-B, collected at Anak Krakatau were chemically analyzed by means of the electron-probe microanalyzer (EPMA). Electron-probe microanalyses of olivines, clinopyroxenes and orthopyroxenes were determined by the general method and corrected by the Bence-Albee method, and those of plagioclases were measured by the rapid method proposed by YUSA (1975).

The electron-probe microanalyses of phenocrystic olivines, clinopyroxenes and orthopyroxenes are tabulated in Tables 7, 8 and 9, respectively, together with their respective structural formulas. The structural formulas were calculated on the basis of 4 oxygens per formula unit for olivine, and 6 oxygens per formula unit for clinopyroxene and orthopyroxene. Anorthite-contents of phenocrystic plagioclases, represented by the anorthite molecular percent for core and rim of the zoned phenocryst, are given in Table 10, together with types of zonning.

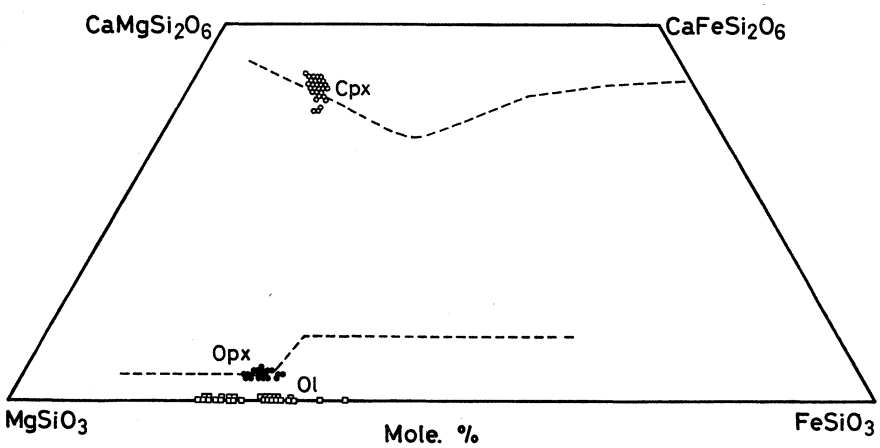

Fig. 9. Plots of the analyzed phenocrystic olivines, clinopyroxenes and orthopyroxenes of volcanic rocks from Anak Krakatau on BROWN's (1957) diagram showing the Skaergaard pyroxene trends (dashed lines). Symbols: open squares, open circles and solid circles represent olivines, clinopyroxenes and orthopyroxenes, respectively.

As a result, the analyzed phenocrystic olivines, clinopyroxenes and orthopyroxenes are, as seen from Fig. 9, similar in composition to phenocrystic olivines, clinopyroxenes and orthopyroxenes of volcanic rocks of island arcs (e.g., NICHOLLS, 1971), as well as those of basaltic and andesitic rocks of oceanic islands (e.g., CARMICHAEL, 1967).

(1) Olivines

The analyzed phenocrystic olivines range in composition from Fa_{22} (chrysolite) to Fa_{39} (hyalosiderite) (see Fig. 9). An individual phenocrysts of olivine show zonning. The compositional variation is less than 5 mole. % in the component of fayalite within the zoned olivines. Meanwhile, phenocrystic olivines of the volcanic bomb (sample no. 702-A) have slightly normal zone in compositional change (see nos. 1 and 3 in Table 7). In the NiO-content, the analyzed phenocrystic olivines are lower than phenocrystic olivines of basaltic rocks of oceanic islands (e.g., MOORE and EVANS, 1967).

(2) Clinopyroxenes

The analyzed phenocrystic clinopyroxenes range in composition from $Wo_{44}Fs_{12}$ to $Wo_{38}Fs_{17}$; that is, they belong to augite according to the classification of clinopyroxenes by POLDERVAART and HESS (1951). The compositional variation is less than 5 mole. % in the components of wollastonite and clinoferrosilite within the zoned augite grains. A tendency of a slight decreasing of the wollastonite-component, and, in contrast, a tendency of a slight increasing of the clinoferrosilite-component, from core towards rim, are as a whole recognized in the individual augite grains (see sample nos. 605 and 702-B in Table 8). The values of the Fe^{2+}/Mg ratios are fairly uniform throughout the analyzed phenocrystic augites of the volcanic rocks from Anak Krakatau. In the contents of Al_2O_3 and Cr_2O_3, most of the analyzed phenocrystic augites are much lower as compared to those of phenocrystic clinopyroxenes of basaltic rocks of oceanic islands (e.g., CARMICHAEL, 1967).

(3) Orthopyroxenes

The analyzed phenocrystic orthopyroxenes range in composition from Fs_{26} (bronzite) to Fs_{31} (hypersthene). No zonning can be observed in phenocrystic orthopyroxenes of sample nos. 501, 504 and 605, rocks of lava flows. Microphenocrystic orthopyroxenes of volcanic bomb (sample no. 702-A) have a slight compositional difference grain by grain. A weak normal zonning is found only in phenocrystic orthopyroxenes of a xenolith (sample no. 702-B) from the volcanic bomb, though the compositional variation within the zoned phenocryst is less than 5 mole. % (see Table 9).

(4) Plagioclases

The analyzed plagioclases, large and intermediate phenocrysts is size, of rocks of sample nos. 501, 504 and 605, lava flows, and sample no. 720-A, volcanic bomb, range in composition from An_{83} (bytownite) to An_{59} (labradorite) (Fig. 10, left); and those of a xenolith (sample no. 702-B) from the volcanic bomb range in composition from An_{90} (bytownite) to An_{67} (laboradorite) (Fig. 10, right). The anorthite-composition of microphenocrystic plagioclases were also measured to be $An_{70}\sim An_{55}$. Most of the

Table 7. Electron-probe microanalyses of olivines from volcanic rocks of the Anak Krakatau

Rock No.	501						504						605		
No.	1		2		3		1		2		3		1		2
	Core	Rim	Core	Rim	Core	Rim	Core	Rim	Core	Rim	Core	Rim	Core	Rim	Core
SiO_2	37.34	37.30	37.54	37.10	36.99	36.87	37.79	38.30	38.50	39.01	37.62	37.70	37.50	37.69	38.59
TiO_2	0.03	0.04	0.04	0.01	0.01	0.06	0.02	tr.	tr.	tr.	0.03	tr.	0.04	0.01	tr.
Al_2O_3	0.07	0.06	0.10	0.08	0.10	0.16	0.05	0.05	0.11	0.04	0.09	0.07	0.06	0.05	0.06
FeO*	26.44	27.56	26.98	28.81	28.40	29.23	23.63	23.33	20.79	21.25	26.27	25.55	26.17	27.12	20.88
MnO	0.54	0.55	0.51	0.61	0.56	0.59	0.45	0.39	0.43	0.33	0.53	0.54	0.49	0.82	0.38
MgO	35.63	34.74	34.51	33.80	33.37	33.37	37.50	38.27	39.73	39.84	35.07	35.09	34.96	33.87	39.11
CaO	0.19	0.20	0.31	0.19	0.20	0.20	0.17	0.17	0.17	0.18	0.19	0.18	0.20	0.22	0.18
NiO	0.11	0.15	0.10	0.12	0.12	0.09	0.12	0.10	0.08	0.13	0.09	0.10	0.10	0.12	0.11
Total	100.35	100.60	100.09	100.72	99.75	100.57	99.73	100.61	99.81	100.78	99.89	99.23	99.52	99.90	99.31
Si	0.990	0.992	1.000	0.992	0.997	0.989	0.994	0.996	0.997	1.001	0.998	1.006	1.001	1.007	1.005
Al	0.002	0.002	0.003	0.003	0.003	0.005	0.002	0.002	0.003	0.001	0.003	0.002	0.002	0.002	0.002
Ti	0.001	0.001	0.001	tr.	tr.	0.001	tr.	tr.	tr.	tr.	0.001	tr.	0.001	tr.	tr.
Mg	1.409	1.377	1.370	1.347	1.340	1.335	1.471	1.483	1.534	1.525	1.387	1.396	1.391	1.349	1.518
Fe^{+2}	0.586	0.613	0.601	0.644	0.640	0.656	0.520	0.507	0.450	0.456	0.593	0.570	0.584	0.606	0.455
Mn	0.012	0.012	0.012	0.014	0.013	0.013	0.010	0.009	0.009	0.007	0.012	0.012	0.011	0.019	0.008
Ca	0.005	0.006	0.009	0.005	0.006	0.006	0.005	0.005	0.005	0.005	0.005	0.005	0.006	0.006	0.005
Ni	0.002	0.003	0.002	0.003	0.003	0.002	0.003	0.002	0.002	0.003	0.002	0.002	0.002	0.003	0.002

Table 7. (Continued)

Rock No.	605			702-A						702-B					
No.	2	3		1		2		3		1		2		3	
	Rim	Core	Rim	Core	Rim	Core	Rim	Core	Rim	Core	Rim	Core	Rim	Core	Rim
SiO_2	38.37	37.31	37.26	36.27	36.13	38.04	37.88	38.46	38.49	37.22	37.15	36.99	37.28	37.23	37.35
TiO_2	0.01	0.01	0.05	0.06	0.02	tr.	tr.	0.01	0.01	tr.	0.02	0.01	0.01	0.02	0.03
Al_2O_3	0.05	0.07	0.13	0.21	0.13	0.11	0.07	0.13	0.11	0.16	0.13	0.07	0.07	0.08	0.06
FeO*	20.08	26.44	26.28	31.09	33.46	23.48	23.80	21.00	24.43	27.40	27.46	27.37	27.53	26.47	26.27
MnO	0.31	0.53	0.51	0.58	0.65	0.43	0.44	0.32	0.39	0.74	0.70	0.75	0.74	0.78	0.77
MgO	39.93	34.67	35.32	30.75	29.35	38.31	37.54	40.01	36.97	34.58	34.29	34.61	34.58	34.90	34.86
CaO	0.19	0.18	0.21	0.25	0.26	0.17	0.17	0.19	0.20	0.18	0.18	0.16	0.18	0.17	0.17
NiO	0.09	0.11	0.12	0.13	0.11	0.14	0.13	0.08	0.08	0.14	0.12	0.10	0.14	0.08	0.12
Total	99.03	99.32	99.88	99.34	100.11	100.68	100.03	100.20	100.68	100.52	100.05	100.06	100.53	99.73	99.63
Si	0.999	1.000	0.992	0.996	0.996	0.990	0.994	0.993	1.004	0.993	0.994	0.990	0.993	0.995	0.998
Al	0.001	0.002	0.004	0.007	0.004	0.003	0.002	0.004	0.003	0.005	0.004	0.002	0.002	0.003	0.002
Ti	tr.	tr.	0.001	0.001	tr.	tr.	tr.	tr.	tr.	tr.	tr.	tr.	tr.	tr.	0.001
Mg	1.549	1.385	1.402	1.258	1.251	1.486	1.469	1.540	1.438	1.372	1.367	1.381	1.373	1.390	1.388
Fe^{+2}	0.473	0.593	0.585	0.714	0.771	0.511	0.522	0.454	0.533	0.610	0.614	0.613	0.613	0.592	0.587
Mn	0.007	0.012	0.012	0.014	0.015	0.010	0.010	0.007	0.009	0.017	0.016	0.017	0.017	0.018	0.017
Ca	0.005	0.005	0.006	0.007	0.008	0.005	0.005	0.005	0.006	0.005	0.005	0.005	0.005	0.005	0.005
Ni	0.002	0.002	0.003	0.003	0.002	0.003	0.003	0.002	0.002	0.003	0.003	0.002	0.003	0.002	0.003

* Total Fe as FeO.
Structural formulas are calculated on the basis of 4 oxygens.

Table 8. Electron-probe microanalyses of clinopyroxenes from volcanic rocks of the Anak Krakatau

Rock No.	501						504						605		
No.	1		2		3		1		2		3		1		2
	Core	Rim	Core	Rim	Core	Rim	Core	Rim	Core	Rim	Core	Rim	Core	Rim	Core
SiO_2	50.37	51.00	51.66	50.89	51.55	51.65	51.84	51.56	51.11	51.47	51.32	51.74	51.19	51.63	50.54
TiO_2	0.78	0.82	0.72	0.76	0.56	0.60	0.67	0.70	0.72	0.69	0.56	0.71	0.67	0.68	0.45
Al_2O_3	2.40	2.52	2.12	2.15	1.45	1.62	1.96	2.07	2.15	2.16	1.76	1.80	2.31	1.98	2.54
Cr_2O_3	0.04	tr.	0.03	0.01	0.01	0.01	0.03	0.02	0.02	0.04	0.02	0.02	0.03	0.02	0.19
FeO*	9.58	10.37	8.98	9.48	10.03	9.67	9.31	10.51	9.34	9.03	9.81	9.12	8.66	9.31	7.69
MnO	0.33	0.44	0.36	0.40	0.43	0.41	0.37	0.38	0.34	0.30	0.49	0.41	0.39	0.36	0.29
MgO	15.54	15.64	15.38	15.12	16.19	15.72	15.29	15.32	15.33	15.66	14.95	15.48	15.40	15.50	15.64
CaO	19.86	18.77	20.41	20.19	18.99	19.69	20.45	19.67	20.30	20.54	20.77	20.78	21.34	20.68	21.57
Na_2O	0.26	0.27	0.26	0.28	0.22	0.27	0.28	0.29	0.28	0.25	0.30	0.27	0.27	0.27	0.24
Total	99.16	99.83	99.92	99.28	99.43	99.64	100.20	100.52	99.59	100.14	99.98	100.33	100.26	100.43	99.15
Si	1.899	1.908	1.925	1.915	1.934	1.933	1.929	1.920	1.915	1.915	1.924	1.924	1.906	1.919	1.898
Al^{IV}	0.101	0.092	0.075	0.085	0.064	0.067	0.071	0.080	0.085	0.085	0.076	0.076	0.094	0.081	0.102
Z	2.000	2.000	2.000	2.000	1.998	2.000	2.000	2.000	2.000	2.000	2.000	2.000	2.000	2.000	2.000
Al^{VI}	0.006	0.019	0.018	0.010	-	0.004	0.015	0.011	0.010	0.010	0.002	0.003	0.007	0.006	0.010
Ti	0.022	0.023	0.020	0.022	0.014	0.017	0.019	0.020	0.020	0.019	0.016	0.020	0.019	0.019	0.013
Cr	0.001	tr.	0.001	tr.	tr.	tr.	0.001	0.001	0.001	0.001	0.001	0.001	0.001	0.001	0.006
Mg	0.873	0.872	0.854	0.848	0.905	0.877	0.848	0.850	0.856	0.869	0.835	0.858	0.855	0.859	0.875
Fe^{+2}	0.302	0.324	0.280	0.298	0.315	0.303	0.290	0.327	0.293	0.281	0.308	0.284	0.270	0.289	0.242
Mn	0.011	0.014	0.011	0.013	0.014	0.013	0.012	0.012	0.011	0.010	0.016	0.013	0.012	0.011	0.009
Ca	0.802	0.752	0.815	0.814	0.763	0.790	0.815	0.785	0.815	0.819	0.834	0.828	0.851	0.824	0.868
Na	0.019	0.020	0.019	0.020	0.016	0.020	0.020	0.021	0.020	0.018	0.022	0.020	0.020	0.020	0.018
X	2.036	2.024	2.018	2.025	2.027	2.024	2.020	2.027	2.026	2.027	2.034	2.027	2.035	2.029	2.041

Table 8. (Continued)

Rock No.	605			702-A						702-B					
No.	2	3		1		2		3		1		2		3	
	Rim	Core	Rim	Core	Rim	Core	Rim	Core	Rim	Core	Rim	Core	Rim	Core	Rim
SiO_2	51.30	51.10	51.62	51.01	51.68	52.10	51.45	51.67	51.26	51.71	50.55	51.76	52.17	51.31	50.81
TiO_2	0.59	0.66	0.75	0.85	0.69	0.67	0.63	0.64	0.70	0.85	0.65	0.79	0.76	0.49	0.51
Al_2O_3	1.88	2.35	2.08	2.24	2.10	2.07	1.97	2.10	2.39	2.71	1.93	2.51	2.32	1.88	2.69
Cr_2O_3	0.02	0.02	0.02	0.06	0.01	0.02	0.04	0.03	0.04	0.01	0.01	tr.	0.02	0.01	0.02
FeO*	9.29	8.79	10.12	9.47	9.11	8.84	10.05	8.92	10.01	8.83	9.49	8.47	8.95	8.96	9.27
MnO	0.36	0.34	0.40	0.33	0.31	0.32	0.40	0.43	0.28	0.38	0.38	0.41	0.41	0.50	0.45
MgO	15.57	15.41	15.26	15.19	15.62	15.59	15.51	15.11	14.67	15.17	15.50	15.30	15.40	14.86	15.29
CaO	20.21	20.97	19.78	20.52	20.56	20.66	18.87	20.52	20.07	20.84	20.42	20.94	20.02	20.98	20.24
Na_2O	0.28	0.26	0.30	0.27	0.28	0.27	0.26	0.26	0.26	0.29	0.25	0.30	0.29	0.29	0.26
Total	99.50	99.90	100.33	99.94	100.36	100.54	99.18	99.68	99.68	100.79	99.18	99.72	100.34	99.28	99.54
Si	1.923	1.908	1.923	1.908	1.919	1.927	1.933	1.930	1.921	1.910	1.908	1.916	1.931	1.930	1.905
Al^{IV}	0.077	0.092	0.077	0.092	0.081	0.073	0.067	0.070	0.079	0.090	0.086	0.084	0.069	0.070	0.095
Z	2.000	2.000	2.000	2.000	2.000	2.000	2.000	2.000	2.000	2.000	1.994	2.000	2.000	2.000	2.000
Al^{VI}	0.006	0.011	0.014	0.007	0.011	0.017	0.020	0.023	0.027	0.028	-	0.026	0.032	0.013	0.024
Ti	0.017	0.019	0.021	0.024	0.019	0.019	0.018	0.018	0.020	0.024	0.012	0.022	0.021	0.014	0.014
Cr	0.001	0.001	0.001	0.002	tr.	0.001	0.001	0.001	0.001	tr.	tr.	tr.	0.001	tr.	0.001
Mg	0.870	0.858	0.847	0.847	0.865	0.860	0.869	0.841	0.820	0.835	0.872	0.844	0.850	0.833	0.855
Fe^{+2}	0.291	0.275	0.315	0.296	0.283	0.274	0.316	0.279	0.314	0.273	0.300	0.262	0.277	0.282	0.291
Mn	0.011	0.011	0.013	0.011	0.010	0.010	0.013	0.014	0.009	0.012	0.012	0.013	0.013	0.016	0.014
Ca	0.812	0.839	0.789	0.822	0.818	0.819	0.760	0.821	0.806	0.825	0.826	0.830	0.794	0.846	0.813
Na	0.020	0.019	0.022	0.020	0.020	0.019	0.019	0.019	0.019	0.021	0.018	0.022	0.021	0.021	0.019
X	2.028	2.033	2.022	2.029	2.026	2.019	2.016	2.016	2.016	2.018	2.040	2.019	2.009	2.025	2.031

* Total Fe as FeO.

Structural formulas are calculated on the basis of 6 oxygens.

Table 9. Electron-probe microanalyses of orthopyroxenes from volcanic rocks of the Anak Krakatau

Rock No.	501				504				605			
No.	1		2		1		2		1		2	
	Core	Rim	Core	Rim	Core	Rim	Core	Rim	Core	Rim	Core	Rim
SiO_2	53.87	53.90	53.63	53.29	54.22	54.06	53.47	52.70	53.53	53.13	53.44	53.47
TiO_2	0.31	0.31	0.33	0.29	0.40	0.36	0.32	0.44	0.37	0.29	0.34	0.43
Al_2O_3	0.83	1.20	0.83	0.93	1.00	1.13	1.23	1.15	1.01	1.17	0.90	1.18
Cr_2O_3	0.02	tr.	tr.	tr.	0.02	0.02	0.01	0.01	0.02	0.02	0.02	0.02
FeO*	18.10	17.48	18.06	17.58	17.36	17.47	17.48	17.68	18.01	17.94	17.82	18.01
MnO	0.84	0.51	0.83	0.61	0.54	0.51	0.68	0.55	0.61	0.55	0.58	0.56
MgO	25.01	25.05	24.81	24.85	25.37	25.45	24.95	24.67	24.82	24.70	25.00	24.54
CaO	1.55	1.85	1.56	1.67	1.75	1.70	1.74	2.00	1.83	1.87	1.83	2.00
Na_2O	0.04	0.04	0.04	0.03	0.04	0.04	0.04	0.04	0.05	0.04	0.05	0.05
Total	100.57	100.34	100.09	99.25	100.70	100.74	99.92	99.24	100.25	99.71	99.98	100.26
Si	1.965	1.962	1.965	1.965	1.965	1.960	1.957	1.948	1.958	1.954	1.959	1.956
Al^{IV}	0.035	0.038	0.035	0.035	0.035	0.040	0.043	0.050	0.042	0.046	0.039	0.044
Z	2.000	2.000	2.000	2.000	2.000	2.000	2.000	1.998	2.000	2.000	1.998	2.000
Al^{VI}	0.001	0.014	0.001	0.005	0.008	0.008	0.010	-	0.002	0.005	-	0.007
Ti	0.009	0.009	0.009	0.008	0.011	0.010	0.009	0.012	0.010	0.008	0.009	0.012
Cr	0.001	tr.	tr.	tr.	0.001	0.001	tr.	tr.	0.001	0.001	0.001	0.001
Mg	1.360	1.360	1.355	1.366	1.371	1.375	1.362	1.359	1.354	1.354	1.366	1.338
Fe^{+2}	0.552	0.532	0.554	0.542	0.526	0.530	0.535	0.547	0.551	0.552	0.546	0.551
Mn	0.026	0.016	0.026	0.019	0.017	0.016	0.021	0.017	0.019	0.017	0.018	0.017
Ca	0.061	0.072	0.061	0.066	0.068	0.066	0.068	0.079	0.072	0.074	0.072	0.078
Na	0.003	0.003	0.003	0.002	0.003	0.003	0.003	0.003	0.004	0.003	0.004	0.004
X	2.013	2.006	2.009	2.008	2.005	2.009	2.008	2.017	2.013	2.014	2.016	2.008

Rock No.	702-A				702-B					
No.	1	2	3	4	1		2		3	
					Core	Rim	Core	Rim	Core	Rim
SiO_2	54.27	53.69	52.40	53.71	53.37	52.47	54.32	53.12	52.85	53.98
TiO_2	0.25	0.32	0.42	0.30	0.25	0.37	0.41	0.36	0.43	0.29
Al_2O_3	0.61	0.92	1.42	0.73	1.15	1.01	0.92	1.42	1.40	0.93
Cr_2O_3	0.02	0.02	tr.	0.02	0.01	0.02	0.04	0.04	0.02	0.02
FeO*	17.48	16.93	19.04	17.67	16.63	19.66	17.10	18.02	17.01	18.55
MnO	0.66	0.64	0.85	0.57	0.70	0.65	0.69	0.70	0.50	0.61
MgO	25.05	26.12	24.34	25.18	25.65	23.45	25.45	24.95	24.62	23.39
CaO	1.57	1.71	1.59	2.22	1.51	1.79	1.55	1.66	2.03	1.76
Na_2O	0.03	0.05	0.06	0.06	0.05	0.04	0.04	0.06	0.05	0.05
Total	99.94	100.40	100.12	100.46	99.32	99.46	100.52	100.33	98.91	99.58
Si	1.983	1.952	1.933	1.960	1.958	1.953	1.970	1.943	1.952	1.988
Al^{IV}	0.017	0.039	0.062	0.031	0.042	0.044	0.030	0.057	0.048	0.012
Z	2.000	1.991	1.995	1.991	2.000	1.997	2.000	2.000	2.000	2.000
Al^{VI}	0.009	-	-	-	0.008	-	0.009	0.004	0.013	0.028
Ti	0.007	0.009	0.012	0.008	0.007	0.010	0.011	0.010	0.012	0.008
Cr	0.001	0.001	tr.	0.001	tr.	0.001	0.001	0.001	0.001	0.001
Mg	1.364	1.416	1.339	1.370	1.403	1.301	1.376	1.360	1.356	1.284
Fe^{+2}	0.534	0.515	0.588	0.539	0.510	0.612	0.519	0.551	0.526	0.571
Mn	0.020	0.020	0.027	0.018	0.022	0.021	0.021	0.022	0.016	0.019
Ca	0.062	0.067	0.063	0.087	0.059	0.071	0.060	0.065	0.080	0.070
X	1.997	2.028	2.029	2.023	2.009	2.016	1.997	2.013	2.004	1.981

* Total Fe as FeO.

Structural formulas are calculated on the basis of 6 oxygens.

Table 10. Composition of plagioclases from volcanic rocks of the Anak Krakatau

Rock No.	No.	An% of Core*	An% of Rim*	Range in An%*	Zoning	Remarks
501	1	70	68	76-62	Oscillatory	Large in size
	2	71	71	72-68		Intermediate in size
	3	67	66	67-59		Small in size
504	1	70	69	82-69	Oscillatory	Large in size
	2	59	71	76-59	Reverse oscillatory	Intermediate in size
	3	65	70	70-64		Small in size
605	1	82	61	83-61	Normal oscillatory	Large in size
	2	72	73	76-67		Intermediate in size
	3	56	57	55-57		Small in size
702-A	1	72	67	77-59	Slightly normal oscillatory	Large in size
	2	78	64	82-64	Normal oscillatory	Intermediate in size
	3	70	65	70-65		Small in size
702-B	1	89	90	90-79	Oscillatory	Large in size
	2	73	67	73-67		Intermediate in size
	3	59	70	70-55	Reverse	Small in size

* Anorthite mole per cent.

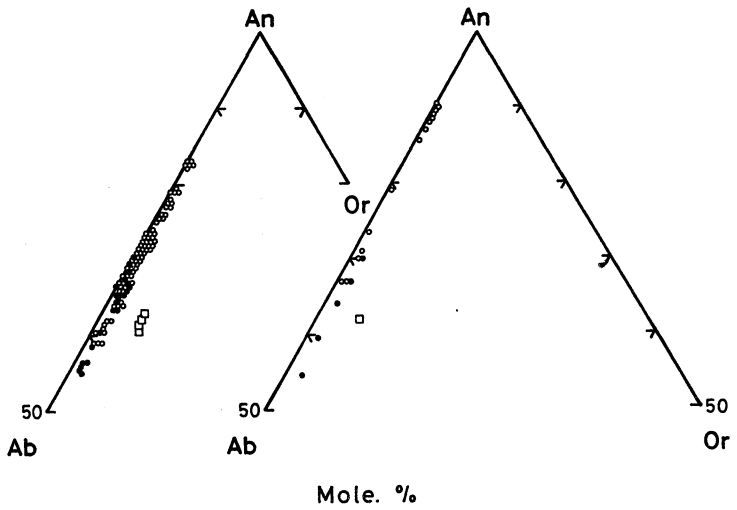

Fig. 10. Plots of the analyzed phenocrystic plagioclases of volcanic rocks from Anak Krakatau on the Ab-Or-An diagrams. Left, plots of plagioclases of rocks of lava flows and a volcanic bomb; right, plots of plagioclases of a xenolith from the volcanic bomb. Symbols: open circles represent plagioclases of large and intermediate phenocrysts in size; and solid circles represent microphenocrystic plagioclases.

analyzed phenocrystic plagioclases are oscilatory in the type of zonning.

Mineralogy

X-ray powder diffraction analysis and observation by the scanning electron microscope were made of thermally altered products and related minerals, and the yellow-colored and stratified pyroclastics from Anak Krakatau, and the matrices of pumice fall and pyroclastic flow from Small Rakata and Sertung.

1. Thermally Altered Products and Related Minerals from Anak Krakatau

A natroalunite (sample no. 505) occurs as masses of white-colored platy crystals on the surface of lava flows, where rocks were affected by solfataric alteration. Relative atomic percent of Na of the naturoalunite is very high. X-ray powder diffraction patterns of the natroalunite is shown in Fig. 11, including those of synthetic natroalunite and synthetic alunite for comparison. X-ray powder data are listed in Table 11, together with those of natural and synthetic natroalunites. From the powder data,

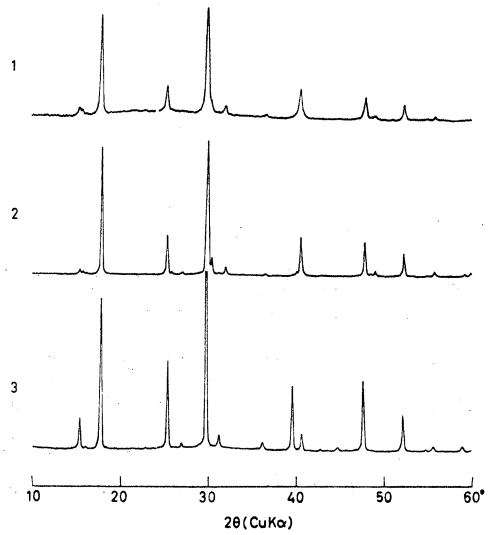

Fig. 11. X-ray powder diffraction patterns for natroalunite from Anak Krakatau (1), synthetic natroalunite (2) and synthetic alunite (3).

Table 11. X-ray diffraction data for natural and synthetic natroalunite

	1	2		3		4	
hkl	d(Å)	d(Å)	I	d(Å)	I	d(Å)	I
101	5.68	5.68	8	5.68	3	5.69	12
003	5.58	5.58	6	5.58	4	5.58	12
012	4.90	4.90	92	4.90	95	4.90	76
110	3.485	3.49	26	3.49	30	3.49	24
104	3.438						
021	2.97	2.98	86	2.97	70	2.97	70
113	2.955	2.96	100	2.96	100	2.96	100
015	2.926	2.93	14	2.93	13	2.93	17
006	2.788	2.788	10	2.79	6	2.79	17
024	2.447						
205							
107	2.222	2.221	28	2.220	30	2.221	48
122	2.201	2.204	9			2.202	12
300	2.012						
214	2.003						
018	1.976						
033	1.893	1.896	26	1.898	26	1.894	29
027	1.874	1.876	2	1.874	2	1.874	2
009	1.858	1.859	5	1.356	4	1.857	10
220	1.743	1.746	15	1.747	17	1.744	21
208	1.719						
131	1.666						
223	1.663						
119	1.640	1.647	3	1.646	4	1.643	5
306	1.632						
134	1.554	1.554	2				
123	1.542	1.542					
312	1.509						
315	1.497			1.501	2	1.501	5
226	1.478	1.479	3				
0210	1.463	1.462	8	1.463	10	1.463	12

1. Calculated d values using a=6.97Å and c=16.73Å
2. Natroalunite from Anak Krakatau.
3. Synthetic natroalunite.
4. Natroalunite from Big Star deposit, Marysvale, Utah (relative atomic percentages of K and Na are 18 and 82 respectively) (after Parker, 1962).

a=6.97 Å and c=16.73 Å were calculated. Scanning electron microphotograph by JEOL JSM-25SII of the natroalunite crystals is shown in Fig. 17, E.

The results obtained from X-ray studies, differential thermal analysis, scanning electron microscopy and infrared absorption spectra, those of which were carried out for the natroalunite, will be discussed in detail in a separate paper (TOMITA et al., 1982).

White-colored substance from the rock sample of the 1963 lava flow (sample no. 502), thermally altered, which was collected at altitude of 150 m above sea-level, was determined to be gypsum, which occurs as a needle-shaped crystal. A common characteristic of the gypsum is a cracking along cleavage surfaces parallel to the axis of elongation, breaking the crystal into thinner layers like micaceous minerals (Fig. 17, F). Indices of refraction are $\alpha=1.522$ and $\gamma=1.529$. Differential thermal analysis curve for the mineral shows a double low-temperature endothermic peak, corresponding to loss of water in two stages (Fig. 12), that is, loss of $1^1/_2$ molecules to give $CaSO_4 \cdot {}^1/_2H_2O$, and then dehydration to anhydrite.

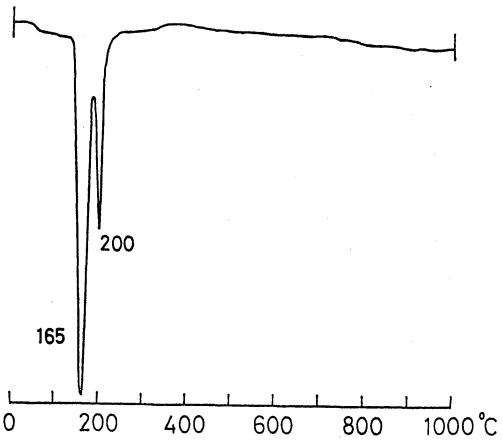

Fig. 12. Differential thermal analysis curve for gypsum from Anak Krakatau.

2. Yellow-colored and Stratified Pyroclastics from Anak Krakatau

The yellow-colored and stratified pyroclastics (sample no. 701) in question, which was collected at a point 701 on the inside wall of the outer cone of Anak Krakatau, were examined by the X-ray powder diffraction method. As a result, none of altered mineral was detected. Observation of the surface of volcanic glass of scoria, which is the major constituent of the yellow-colored and stratified pyroclastics, was made under the scanning electron microscope. The volcanic glass has a number of hole and tube where gases passed through (Fig. 17, G and H).

3. Matrices of Pumice Fall and Pyroclastic Flow from Small Rakata

Fractions less than 2 μm of a fine grained matrix from the pumice fall (sample no. 804) sampled at Small Rakata were collected by the sedimentation method. The fractions dried in air was examined. The X-ray powder diffraction analysis revealed that smectite and halloysite are contained in the sample. Under the scanning electron

microscope, holes and tubes within volcanic glasses of the matrix are well developed. Besides, fractions less than 2 μm of the pyroclastic flow (sample no. 811) from Sertung were also examined by the X-ray powder diffraction method. None of altered mineral was found in the sample.

Summary

1. Geochemical Features of Volcanic Products from the Krakatau Group

Almost all volcanic rocks from the Krakatau Group are basaltic andesites in mineral composition. The volcanic rocks of Anak Krakatau are basaltic andesites, which are common to volcanoes of island arcs, not only in mineral composition but in chemical composition. The plots of the analyzed volcanic rocks fall in a field of KUNO's (1966) high-alumina series on the SiO_2-(Na_2O+K_2O) diagram, and in a field of MIYASHIRO's (1974) tholeiitic series on the SiO_2-total Feo/MgO diagram.

Volcanic rocks and ejecta of Anak Krakatau

Rocks of lava flows and volcanic bomb, collected at Anak Krakatau, apparently represent almost the same characteristic feature not only lithologically but also geochemically, common to baslatic andesites of typical volcanoes of island arcs. Phenocrystic olivines, clinopyroxenes and orthopyroxenes of the rocks of Anak Krakatau are as a whole similar in chemical composition to those of volcanic rocks of island arcs and oceanic islands. The phenocrystic olivines, however, are lower in the NiO-content, and most of the phenocrystic clinopyroxenes are much lower in the Al_2O_3- and Cr_2O_3-contents, as compared to the respective phenocrystic olivines and clinopyroxenes of basaltic rocks of oceanic islands.

A new volcanic ash has some conspicuous difference; the volcanic ash is lower in the SiO_2-content, in other words, it is more basic in composition than others. It is also noted that the volcanic bomb and the enclosing xenolith are higher in the $Fe^{3+}/(Fe^{2+}+Fe^{3+})$ ratio than others.

Volcanic rocks of Small Rakata

Rock of agglutinate lava flow collected at Small Rakata lithologically is olivine-bearing hypersthene-augite andesite, which is characterized by the distinctive structure looking an amygdaloidal pattern under the microscope, with the groundmass giving the pilotaxitic texture. The rock contains xenoliths which are quite the same as augite andesite, collected at Rakata (sample no. 809), characterized by the presence of phenocrystic augite and an intergranular texture of the groundmass. This fact suggests that the xenoliths came from the underlying complex of the Krakatau Volcano before the present Rakata or the ancient Krakatau Volcano.

Volcanic rocks of Rakata

Volcanic rocks of Rakata can lithologically be distinguished into augite-hypersthene andesite and augite andesite, those of which occur as lava flows, and olvine basalt which occurs as dike. It is thought that these three or more rocks make

up the basement complex of Rakata Island. In their groundmasses, augite-hypersthene andesite is characterized by the hyaoliplitic texture, augite andesite by the intergranular texture, and olivine basalt by the intersertal tecture. Besides, it became clear that the rock having been called tridymite andesite is, in mineral composition, augite-hypersthene andesite with cavities filled with tridymite.

2. Detection of Minerals

As a result of X-ray powder diffraction analysis and observation by the scanning electron microscope, natroalunite, i.e., hydrous aluminium sulphate rich in Na, and gypsum were detected from the thermally altered products collected at Anak Krakatau. Meanwhile, it became clear that none of altered mineral is produced in the yellow-colored and stratified pyroclastics, collected on the inside wall of the outer cone of Anak Krakatau, and in the pyroclastic flow collected at Sertung.

3. Physicochemical Nature of Pyroclastic Flow

The pyroclastic flow is characterized by a large amount of volcanic glass in mineral composition, and by the high-contents of silica and alkalies and the low-contents of magnesia, iron oxide and lime in chemical composition; the pyroclastic flow is lithologically andesitic, while geochemically dacitic. It is noted that most volcanic glasses occur in a vesiculating state that vesicles or bubbles and tubes or holes contained in the volcanic glasses are expanding and escaping gases, as shown in Fig. 17, A~D. Such a fact shows that the pyroclastic flow was formed from the "glowing cloud" consisting of fragments and particles which were keeping still high temperature and vesiculating.

4. Petrogenic Significance of Granitic Xenoliths Found from Pyroclastic Flow

Granitic xenoliths of quartz monzonite in mineral composition were found from the pyroclastic flow of Sertung. Only both granitic xenolith and andesitic xenolith have been found from the pyroclastic flow. Granitic xenolith has never been reported from volcanic rocks of the Krakatau Group, and none of granitic rock occurs throughout the whole islands. Therefore, it should be considered that the granitic xenoliths came from the underlying complex at depths, where they were captured as foreign materials by magma.

Meanwhile, the pyroclastic flow significantly differs in both mineral and chemical compositions against all volcanic rocks of the Krakatau Group. The pyroclastic flow would have genetically been related with the underlying granitic complex with respect to the generation of its source magma. The granitic xenoliths found from the pyroclastic flow will be important to discuss the mechanism of its related magma generation.

Acknowledgements

Many thanks are given to Prof. Dr. D. SASTRAPRADJA and Mr. H. NAPITUPULU, Indonensian Institute of Sciences (LIPI); and to Mr. E. SUKARNA, Mr. H. SYAFRUDIN, Ir. M.Z. SJARIFUDIN, Ir. R. PRAPTOWIDJOJO, Mr. SANTOSO and Mr. A.J.T. SIHOMBING, Volcanological Survey of Indonesia (VSI); and to staffs of Geochemical Laboratory, VSI, for their kind acceptance and assistance; and to Prof. G.A. DE NÉVE, Padjadjaran University, for his meaningful discussion. Members of Japanese working group wish to express their appreciation to Indonesian co-workers; they could not proceed successfuly the field work without their great support. Thanks are also given to Mr. H. SAIGŌ for his assistance in preparation of thin sections; to Mr. T. KAMISASANUKI for his technical assistance in analytical study by EPMA; and to Mr. S. KIYOSAKI and Mr. T. ISHII, Kagoshima University, for their assistance in modal analysis. Japanese members gratefully acknowledge for the Japan Society for the Promotion of Sicence (JSPS), from which the financial support in the 1981 fiscal year was provided.

References

BROWN, G.M., 1957, Pyroxenes from the early and middle stages of fractionation of the Skaergaard intrusion, East Greenland. Min. Mag., vol. 31, p. 511–543.

CARMICHAEL, I.S.E., 1967, The mineralogy of Thingmuli, a Tertiary volcano in Eastern Iceland. Amer. Mineral., vol. 52, p. 1841–1851.

CARMICAHEL, I.S.E., TURNER, F.J., and VERHOOGEN, J., 1974, Igneous petrology, 739 p. McGraw-Hill Book Co.

DE NÉVE, G.A., 1981a, Historical notes on Krakatau's eruption of 1883, and activities in previous times. Volcanological Survey of Indonesia, 45 p.

DE NÉVE, G.A., 1981b, Volcanological notes on Krakatau and fifty years of Anak Krakatau. Geosurvey Newsletter, Vol. 13, no. 8, p. 65–71.

ESCHER, B.G., 1919, Excursie-Gids voor Krakatau. Abrecht & Co., Jakarta, 7 p., cited from SUDRADJAT (1981).

EWART, A., 1976, Mineralogy and chemistry of modern orogenic lavas — some statistics and implications. Earth and Planetary Science Letters, vol. 31, p. 417–432.

GEOTIMES, 1979, Geologic events, News notes, vol. 24, no. 12, p. 19–20.

IUGS Subcommission on the Systematics of Igneous Rocks, 1973, Classification and nomemclature of putonic rocks; Recommendations. N. Jahrbuch f. Mineralogie, Heft 4, s. 149–164.

KUNO, H., 1966, Lateral variation of basalt magma type across continental margins and island arcs. Bull. Volcanol., vol. 29, p. 195–222.

MIYASHIRO, A., 1974, Volcanic rocks series in island arcs and active continental margins. Am. Jour. Sci., vol. 274, p. 321–355.

MOORE, J.G., and EVANS, B.W., 1967, The role of olivine in the crystallization of the prehistoric Makaopuhi lava lake, Hawaii. Contr. Mineralogy and Petrology, vol. 15, p. 202–223.

NICHOLLS, I.A., 1971, Petrology of Santorini Volcano, Cyclades, Greece. Jour. Petrology, vol. 12, p. 67–119.

PARKER, R.L., 1962, Isomorphous substitution in natural and synthetic alunite. Amer. Mineral., vol. 47, p. 127–136.

POLDERVAART, A., and HESS, H.H., 1951, Pyroxenes in the crystallization of basaltic magmas. Jour. Geology, vol. 59, p. 472–489.

SUDRADJAT, A., 1981, The morphological development of Krakatau Volcano, Sunda Strait, Indonesia. IAVCEI and Volcanological Survey of Indonesia, 18 p.

TOMITA, K., ŌBA, N., YAMAMOTO, M., ISTIDJAB, M., BADRUDDIN M., SADJIMAN, DJUWANDI, A., and PARLIN, M., 1982, The occurrence of natroalunite at Anak Krakatau, Indonesia.

Reports of Faculty of Science, Kagoshima Univ., no. 15, p. 77–87.
Volcanol. Soc. Japan, and IAVCEI, 1980, Annual report of the world volcanic eruptions in 1978. Bull. Volcanic Eruptions, no. 18, 87 p.
Volcanol. Soc. Japan, and IAVCEI, 1981, Annual report of the world volcanic eruptions in 1979. Bull. Volcanic Eruptions, no. 19, 86 p.
YUSA, Y., 1975, A rapid method for quantitative microprobe analysis of olivines, pyroxenes and feldspars. Jour. Japanese Assoc. Mineralogists, Petrologists, Econ. Geologists, vol. 70, p. 141–156 (in Japanese with English abstract).

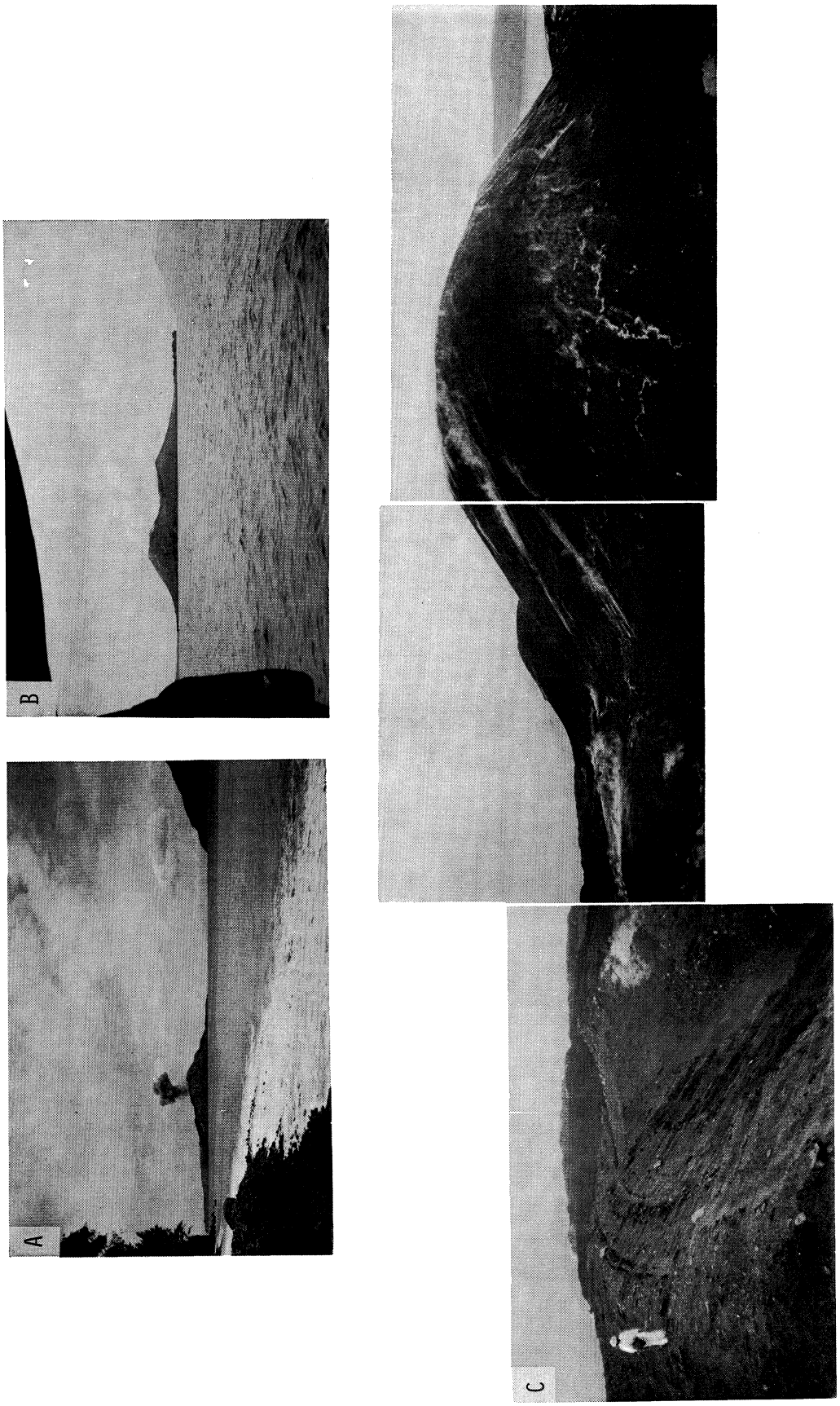

Fig. 13. Anak Karakatau Active Volcano Island.
A. Eruption with smoke at Anak Krakatau active volcano island. Taken at 12:15, Dec. 8, 1981 at Sertung.
B. Anak Krakatau Volcano, a double cone, composed of an inner cone (left), active at present, and an outer cone.
C. Close up of the outer cone (left) with the steep crater wall and the inner cone (right) with many fumaroles at Anak Krakatatu.

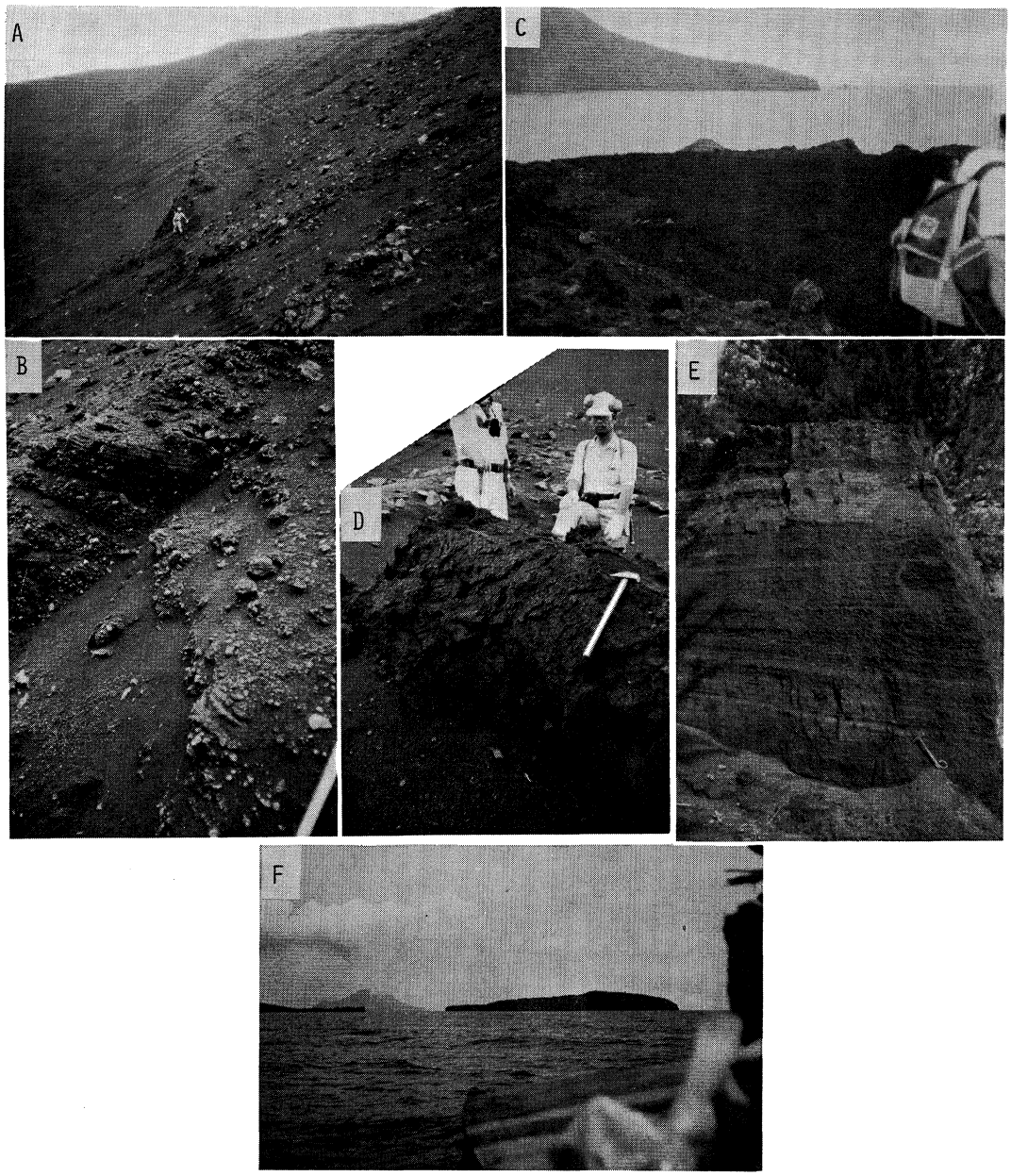

Fig. 14. The yellow-colored and stratified pyroclastics of the outer cone, the 1972–1973 lava flow, the big bread-crust bomb and the fall deposit at Anak Krakatau, and the distance view of Small Rakata Island.

A. The yellow-colored and stratified pyroclastics (sample no. 503) where Dr. Yamamoto stands on the steep crater wall of the outer cone of Anak Krakatau.

B. Close up of the yellow-colored and stratified pyroclastics, mostly scoria, of the former A. The white bar at the lower right corner is the handle of rock hammer.

C. The 1972–1973 lava flow which occurs on the southwestern slope of Anak Krakatau. Island at top left is Rakata.

D. The big bread-crust bomb (sample no. 703) found on the eastern slope of the outer cone of Anak Krakatau.

E. Fall deposit, which is composed mainly of scoria and volcanic sand, observed along the southeastern seacoast of the outer cone of Anak Krakatau.

F. Small Rakata Island, center, and Anak Krakatau, left. Sebesi Island in the background.

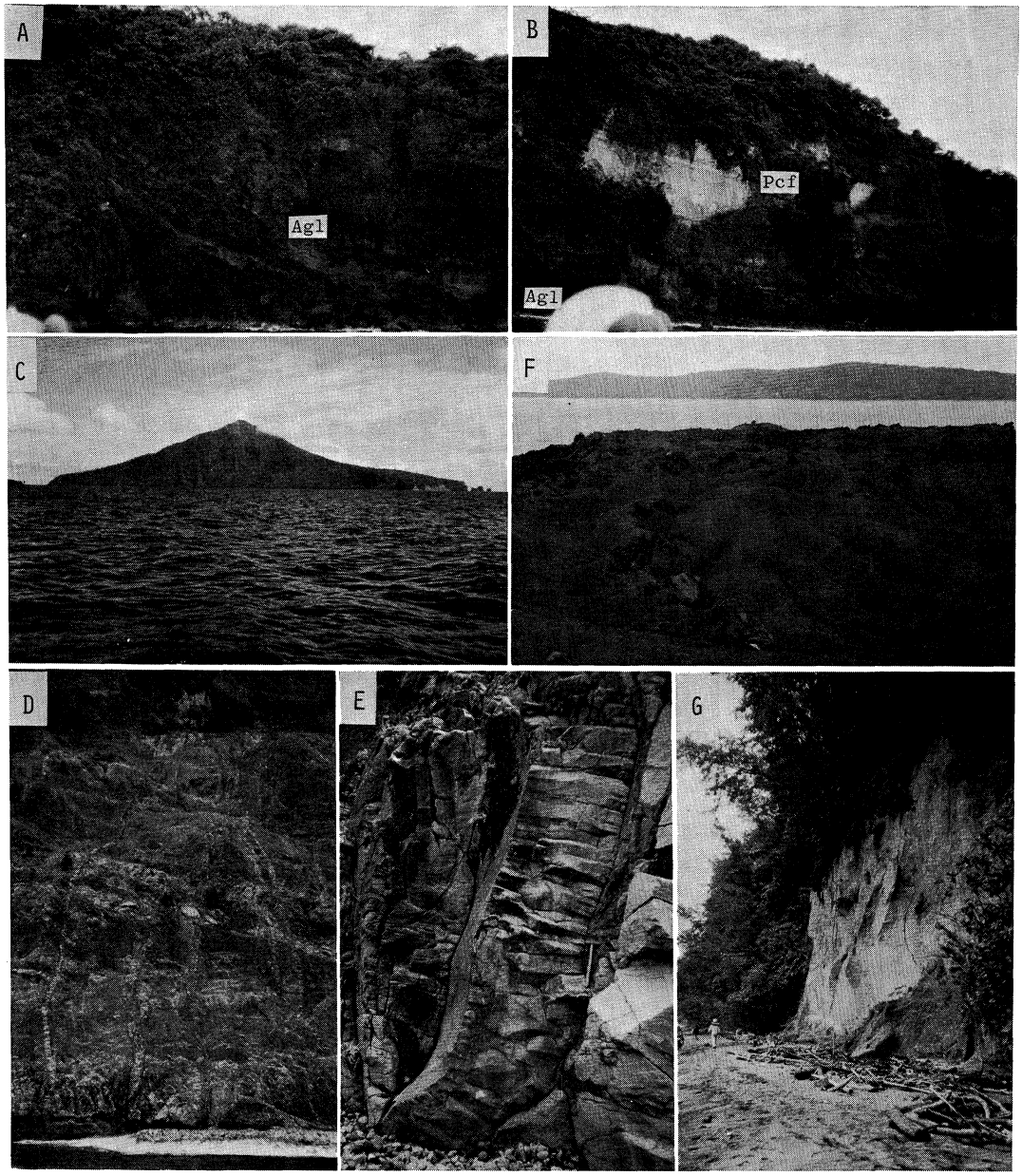

Fig. 15. Agglutinate lava flow and pyroclastic flow at Small Rakata, the distance views of Rakata Island and Sertung Island, many dikes which cut lava flow at Rakata, and the outcrop of pyroclastic flow at Sertung.

A. Agglutinate lava flow (Agl) of olivine-bearing hypersthene-augite andesite (sample no. 805). Taken at Small Rakata.

B. Pyroclastic flow (Pcf) (sample no. 801), the product of the 1883 Krakatau eruption, which overlays pyroclastic deposit. The photograph corresponds to the right handed side of the former A. Taken at Small Rakata. The agglutinate lava flow (Agl) at the left bottom.

C. Rakata Island. Characteristic steeply inclined wall, in the foreground, facing towards Anak krakatau shows the remnant of the 1883 Krakatau explosion.

D. Many dikes which cut lava flow of augite andesite on the steep wall in the NNW-seacoast of Rakata.

E. Close up of the dike of olivine basalt (sample no. 810–A∼C) which cuts the lava flow of augite andesite (sample no. 809).

F. Sertung Island (top), an even and flatted island, and the 1975 (?) lava flow on the western slope of the outer cone of Anak Krakatau (lower).

G. Pyroclastic flow (sample no. 811), ejected in the 1883 Krakatau eruption, that which overlays pumice fall. Lava flow of olivine-hypersthene-augite andesite lies under the pumice fall. Granitic xenolith was found here from the pyroclastic flow. Taken at the southwestern seacoast of Sertung.

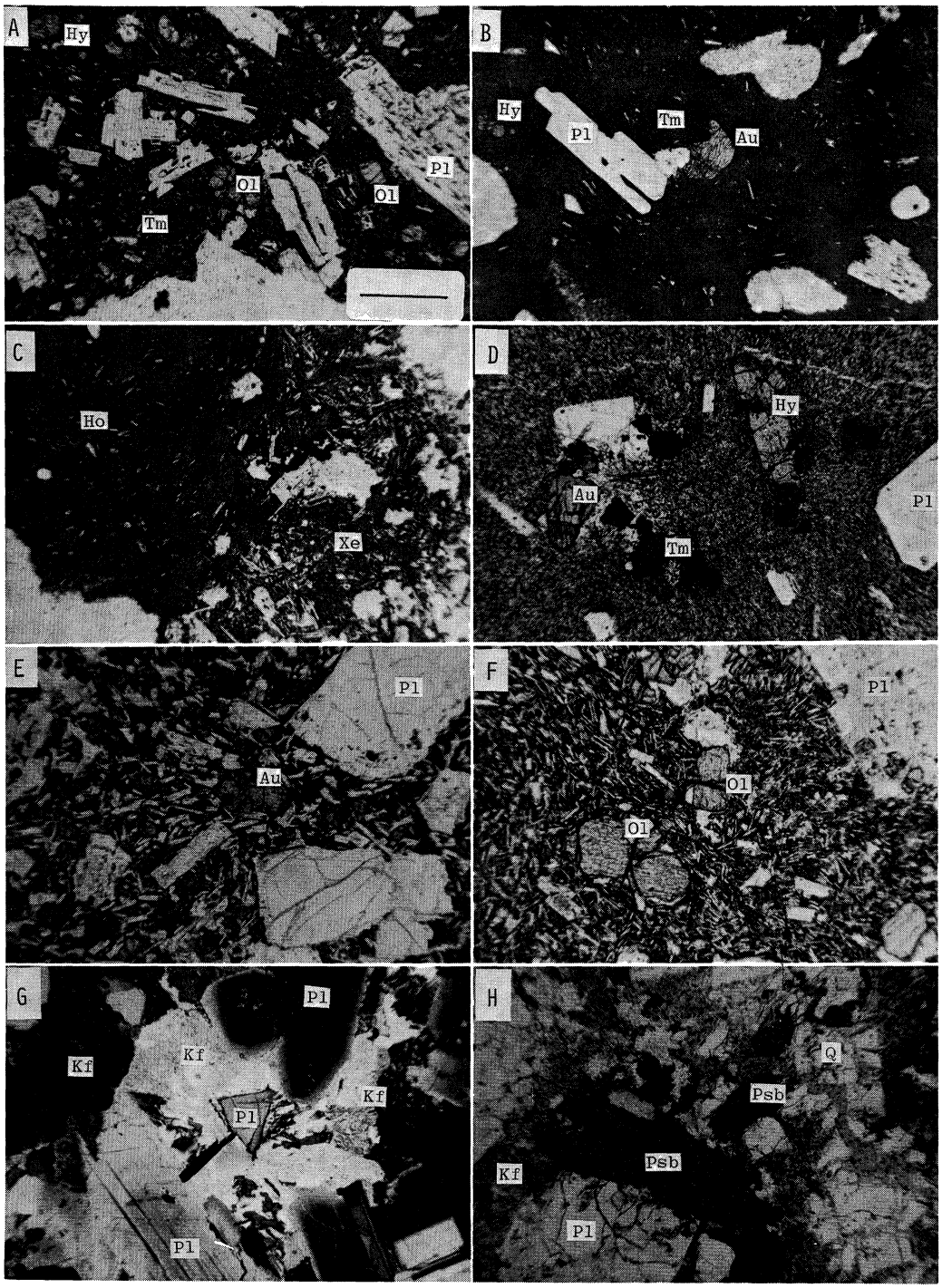
A
Hy
Ol
Ol
Pl
Tm
B
Hy
Pl
Tm
Au
C
Ho
Xe
D
Hy
Au
Pl
Tm
E
Pl
Au
F
Pl
Ol
Ol
G
Pl
Kf
Kf
Kf
Pl
Pl
H
Q
Psb
Psb
Kf
Pl

Fig. 16.

Fig. 16. Microphotographs of volcanic rocks from the Krakatau Group and granitic xenolith found from pyroclastic flow of Sertung. The scale bar in A represents 45 μm; the same scale for all others. Abbreviations: Ol, Olivine; Hy, Hypersthene; Au, Augite; Psb, Pseudomorph after biotite; Pl, Plagioclase; Kf, Potash feldspar; Q, Quartz; Tm, Titanomagnetite.

A. Olivine-bearing hypersthene-augite andesite of 1963 lava flow from Anak Krakatau (sample no. 501).

B. Olivine-bearing hypersthene-augite andesite, which occurs as agglutinate lava flow, from Small Rakata (sample no. 805). Distinctive structure looking amygdaloidal pattern is characteristic.

C. Xenolith (Xe) showing an intergranular texture (right) within the host rock (Ho), sample no. 805.

D. Augite-hypersthene andesite, which has been called tridymite andesite, from Rakata (sample no. 806). The groundmass shows the hyalopilitic texture.

E. Augite andesite (sample no. 809), collected from lava flow at Rakata, showing the intergranular texture.

F. Olivine basalt (sample no. 810-B) of a dike which cuts augite andesite lava flow at Rakata. The groundmass shows the intersertal texture.

G. Well-developed myrmekite, consisting of intergrowth of quartz and plagioclase in the portion where plagioclase abuts on potash feldspar, observed in granitic xenolith (sample no. 811–1) found from pyroclastic flow at Sertung.

H. Pseudomorphs after biotites, showing flakes elongated parallel to basal cleavage, observed in granitic xenolith found from pyroclastic flow of Sertung.

Fig. 17. Scanning electron microphotographs of volcanic glasses (A~D) of pyroclastic flow (sample no. 811) from Sertung, and natroalunite (E), gypsum (F) and scoria (G and H) of the yellow-colored and stratified pyroclastics from Anak Krakatau. The scale bars are 100 μm for A, B, C and G, and 10 μm for D, E, F and H.

A. Volcanic glasses, showing fibrous and vesiculated form, of the pyroclastic flow from Sertung.

B. Close up of fibrous volcanic glass, in which tubes are parallel arranged, locating in the center of the former A.

C. Vesicles and/or holes, where gases passed through, on the cross-section of tubes within volcanic glass of the pyroclastic flow from Sertung.

D. Close up of the vesicles and/or holes developed within the same volcanic glass of the former C.

E. Natrualunite crystals from Anak Krakatau (sample no. 505).

F. Needle-shaped crystals of gypsum from the thermally altered zone at Anak Krakatau (sample no. 502).

G. Holes, where gases passed through, observed on the cross-section of tubes within volcanic glass of scoria of the yellow-colored and stratified pyroclastics (sample no. 701) from Anak Krakatau.

H. Close up of the holes observed in the same volcanic glass of the former G.

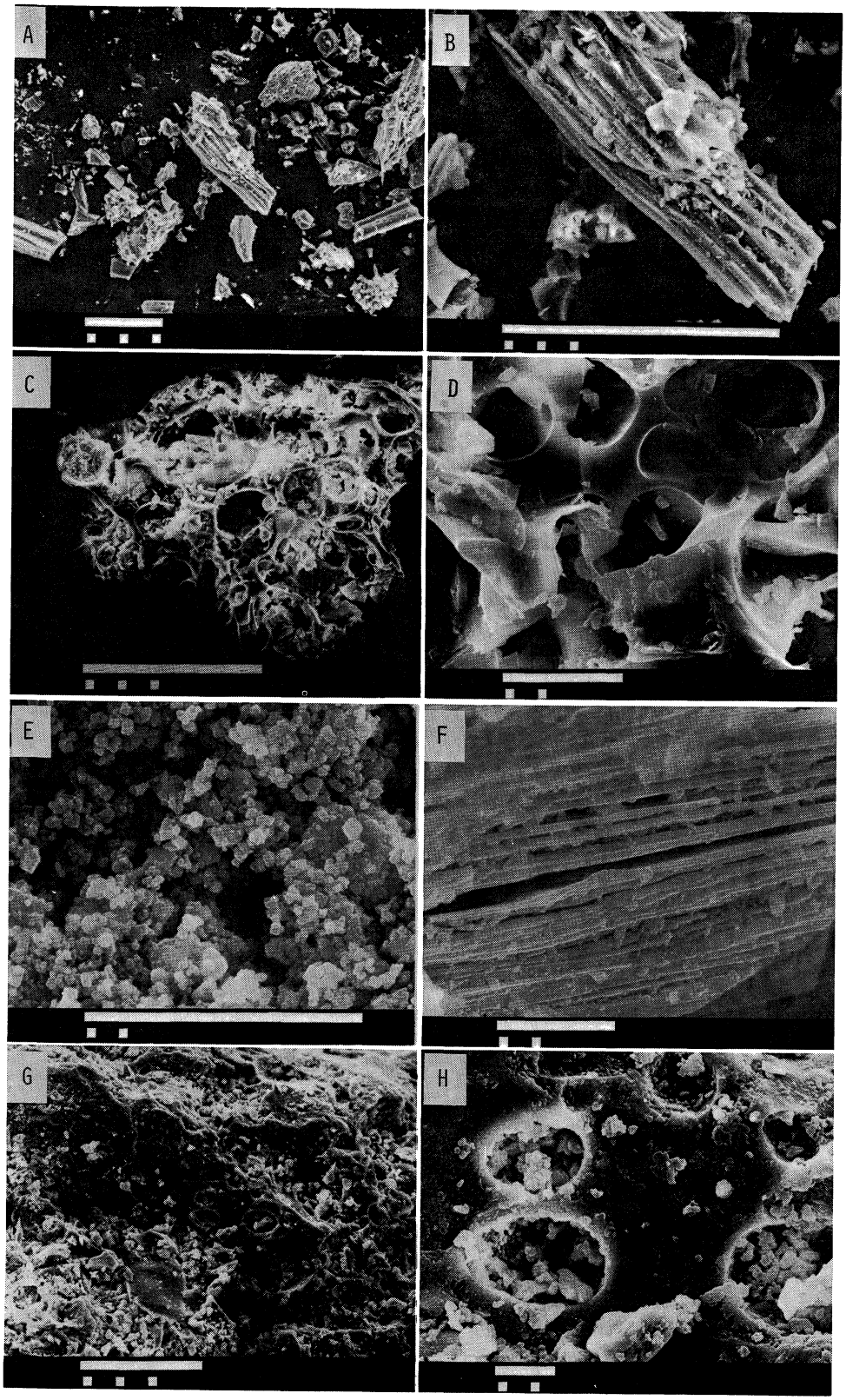

Fig. 17.